Reactor Cooled by High-Temperature Sodium Vapor

W. Van Snyder
August 6, 2024

Abstract

Using new ideas and novel combinations of old ideas, it is possible to construct an inherently and passively safe compact and simple boiling sodium reactor. Fuel is particles of metal nitride ceramic or an alloy containing beryllium or niobium. Liquid sodium coolant enters at the bottom, flows around fuel particles, and sodium vapor exits at the top, circulated by its boiling, not by pumps. The device consists of a reaction region, connected to a storage region in which criticality is impossible. There are no control rods: Power output depends upon the amount of fuel in the reaction region, which is controlled by gas pressure or electromagnetic pumps, and by circulation velocity and void fraction, which are controlled by gas injection. If the gas pressure or electromagnetic pump fails, fuel flows passively under the influence of gravity from the reaction region to the storage region and the reaction stops. The reaction region is small. The volume of circulating coolant is small. Power output can be changed rapidly. If electricity is produced by magnetohydrodynamic generators, the entire plant has essentially no moving parts other than fuel, coolant, and pumps and valves that control gas pressures above the regions. External electrical power is not necessary for safety. Small volumes of fuel slurry are removed continuously for processing, even during shutdown, which reduces or eliminates the "iodine pit" startup control instability. There is no need to shut down the reactor for refueling. The capacity factor should well exceed 95%. Very high burnup is possible.

1 Conceptual outline

The Atomic Energy Commission and especially Oak Ridge National Laboratory were very interested in what they called *Fluid Fuel Reactors*. An enormous variety of them has been described [1]. The present concept bears some superficial resemblance to some of those concepts, but the details here are entirely different from any of them.

In the mobile paste fuel reactor concept described by Atomic Power Development Associates (APDA) in 1961 [2] [3], fuel is a bulk penetrated by coolant tubes rather than fuel being in pins surrounded by flowing coolant.

In the limiting case as coolant tubes become smaller and more numerous, they are eliminated and coolant flows directly through fuel. This concept, which has largely been abandoned, is known as a pebble-bed reactor, a fluidized-bed reactor, or a slurry reactor, depending upon whether coolant flows through a stable bed of fuel particles, levitates them in equilibrium, or carries them away.

Sodium coolant does not react with metallic or metal nitride fuel. It is not necessary to encapsulate fuel in a coating to prevent interaction, as was done in earlier concepts with fuel in contact with coolant. In a fast neutron reactor, it is unnecessary, indeed undesirable, to include a moderator in the fuel particles. This allows to use small fuel particles that are easy to fabricate.

Early homogeneous reactor concepts used aqueous solutions of uranium salts, usually uranyl sulfate, sodium uranyl carbonate, or uranium trifluoride, in heavy water. Those solutions were corrosive. Using water as the coolant required high pressure and low temperature, which complicated construction and reduced thermal efficiency. Water is decomposed by radiation, which required re-combining hydrogen with oxygen, usually used to pre-heat water for the steam generator. Later concepts used molten salts, which also corrode reactor materials. The present concept does not use water directly as a coolant. Actinides and their nitrides do not significantly corrode reactor materials. Therefore, the corrosion problems that prevented progress of those earlier concepts do not exist in the present concept.

The advantage of small uncoated fuel particles is explained in [4]: The surface-to-volume ratio is larger. Inert fission gases do not diffuse through metal. Rather, they move through microcracks and along grain boundaries, or accumulate in sealed pores that eventually expand, interconnect, and break open at the surface. With smaller particles, the distance to the surface from a pore, grain boundary, or microcrack is less. Therefore, it is more likely that a microcrack or grain boundary will initially be directly open to the surface, and there is a smaller limit to the size a sealed pore can attain before it breaks open at the surface:

Small particles expand less than large solid slugs, and endure less thermal strain. Fission products that escape from fuel particles are less likely to be absorbed by small fuel particles [5].

In addition to moving along grain boundaries and microcracks, iodine and many fission-product metals diffuse through fuel, are soluble in sodium [6, Table 1, p. 98], and are insoluble in fuel [7]. Their diffusion rates from fuel into sodium depend upon the surface area. Their production rates depend upon volume. The ratio of diffusion rate to production rate is therefore greater with greater surface-to-volume ratio. The surface-to-volume ratio is greater with smaller particles. With small particles, fission products that are not soluble in sodium also escape directly. With large volumes of coolant flow, coating particles is necessary to prevent contaminating the large volume of coolant with fission products. Section 6 shows that with a small volume of circulating coolant, contamination is a virtue that increases burnup and reduces fuel reprocessing cost.

In a settled paste with uniform-size spherical fuel particles, the maximum fuel density is 74 vol.% $(\pi/\sqrt{18})$.[a] With random close packing, the volume mixing ratio of fuel particles having a polydisperse log normal size distribution with $0 \leq \sigma \leq 3$ is in the range from 60% to 97% [8]. The number of fissions per second is given by $N(t)\,\sigma_f\,\overline{v}\,n(t)$, where $N(t)$ and σ_f are the number density and fission cross section of fissionable atoms, $\overline{v}$ is the average velocity of neutrons, and $n(t)$ is the number of neutrons [9, § 5.2]. With higher volumetric fuel density, specific power output (watts per liter) is larger. Density sufficiently high to cause prompt criticality must be avoided. The density of fuel atoms can be reduced by increasing the proportion of non-fissionable heavy metal or other alloys such as beryllium, niobium, or zirconium.

Fuel composed of very small particles is agitated if coolant flows through it. Depending upon coolant flow rate and state (liquid or gas), the volume fraction of fuel is reduced and the mixture becomes a fluidized bed or a slurry rather than a settled paste. Power output depends upon volume and fuel volume fraction, and therefore upon coolant flow rate and vapor content. Early slurry-fuel reactor concepts assumed the amount of fuel is constant and always within the same container perimeter, with density profiles that depend upon coolant flow conditions. If coolant flow fails, fuel settles into the containment vessel and assumes the density of a solid paste. Oscillations might set in. These cause control instabilities. Most early designs circulated slurry through an external heat exchanger, which required a much larger fuel inventory and complicated shielding, or used an internal heat exchanger, which reduced hydrodynamic efficiency. Therefore, flowing non-boiling slurry-fueled reactor concepts were rejected.

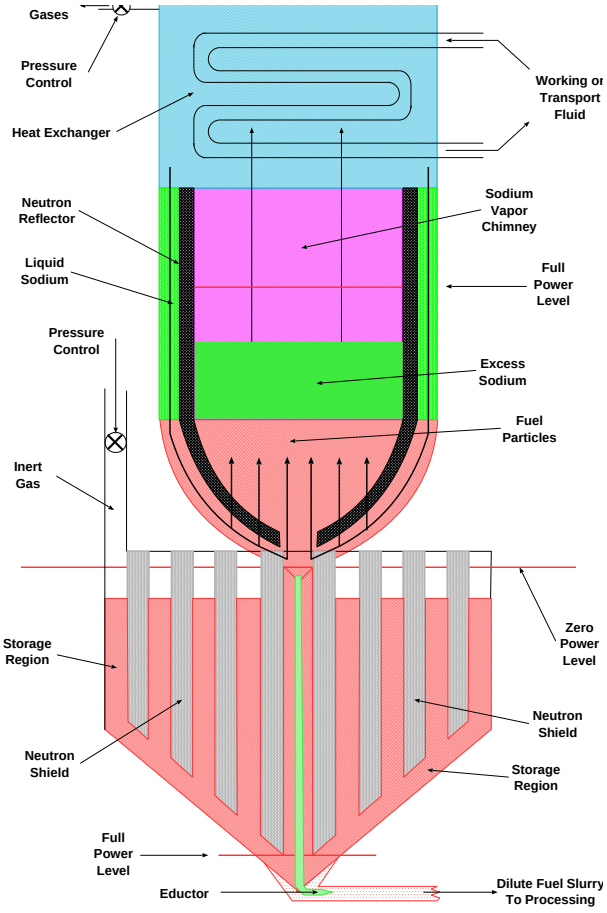

Figure 1: Reactor at Partial Power

The boiling-sodium concept shown in schematic form in Figure 1 is either a pebble-bed, fluidized-bed, or slurry reactor, depending upon particle size and coolant velocity. Coolant velocity depends upon the relationship between the vessel diameter and its power output. There are important distinctions that overcome objections to earlier such concepts: Sodium has much higher heat capacity and thermal conductivity than the gases (usually helium) proposed in those earlier concepts; the enthalpy of vaporization of sodium is large, but gases proposed in those earlier designs did not undergo phase transitions. These phenomena result in a much smaller

[a] This result was conjectured by Johannes Kepler in 1611. Thomas Hales published a proof 10 August 2014.

coolant mass flow rate than in earlier concepts.

This concept embodies two connected regions. Reaction takes place in a compact region that is connected to a storage region in which criticality is impossible, for example, several thin concentric cylindrical shells connected via a conical bottom and separated by neutron shields, shown in cross section in Figure 1. The storage volume is larger than necessary to contain the entire fuel mixture.

Rather than using control rods, power output is determined by the amount of fuel within the reaction region, and the fuel volume fraction, which depends upon coolant velocity [10, p. 65].[b] The bottom of the reaction region is concave (1) to allow operation at low power, (2) to flow fuel toward the connector to the storage region, (3) to control density distribution and thereby eliminate oscillations [11], (4) to reduce neutron leakage, and (5) to produce a decreasing vertical coolant velocity profile. The relationship of the levels of the fuel mixture within the reaction and storage regions is controlled either by the relationship of gas pressures above fuel in the reaction and storage regions, or by electromagnetic pumps.

When pressure is reduced in the storage region, or increased in the reaction region, fuel flows passively, under the influence of gravity, from the reaction region to the storage region, reducing power. This constitutes a negative-reactivity feedback mechanism. Pressure is maintained above the storage region by several redundant normally-open valves that must all be actively closed. Pressure is maintained above the reaction region by an adjustable flow rate valve to remove fission gases from above the heat exchanger. When valves for both regions are open, fuel flows passively, under the influence of gravity, into the storage regions and the reaction region is empty. If fuel particles are sufficiently small to form a viscous paste or colloidal suspension rather than a settled slurry, pressure above the storage region drives fuel into the reaction region. If fuel particles are large, gas pressure above the storage region simply drives sodium through the fuel and into the reaction region; an electromagnetic pump is necessary to lift fuel from the storage region to the reaction region.

The reaction and storage regions, and most of the vapor chimney, are submerged within a sodium pool.

The conversion ratio should be higher and the neutron economy better than in a fixed-fuel reactor because of the absence of structural and fuel cladding materials [10, p. 65].

Fission-induced corrosion might occur, if at all, only in the reactor vessel proper, which could be fitted with an easily-replaceable liner that ought not to need frequent replacement, perhaps made from a ceramic such as beryllia. The strength of most zircaloy and steel alloys is significantly reduced at high temperatures, so the vessel proper must be composed of a material that endures high temperatures and has low neutron absorption cross section, such as a Nb-1%Zr alloy, which melts at 2683°K and has a thermal neutron absorption cross section of 1.155 barns. The outer shell would be cooled by direct contact with sodium flowing downward from the heat exchanger.

2 The reactor in operating condition

In one PRISM design taken as an example [12], the fuel load is 26 tonnes (1,000 kg/T) of uranium with unspecified ^{235}U and ^{239}Pu content, the fuel volume fraction is 28.3%, and the power output is 840 MWth. It was not specified whether the fuel volume fraction is the volume fraction of metallic fuel alloy, or the volume fraction of the interior of fuel pins, about 75% of which is occupied by fuel.[c] Coolant is liquid sodium. The sodium inlet temperature is 360°C (633°K) and the outlet temperature is 499°C (772°K). The coolant flow rate is 5.4 m^3/s = 4,685 kg/s.[d] The average heat capacity of liquid sodium coolant is therefore C_p^ℓ = 840,000 / 4,685 / (772 - 633) = 1.290 kJ/kg/°K. Fuel is contained within pins; sodium coolant is not contaminated with fission products (unless a fuel pin ruptures).

Assuming the volume fraction for random close packing of uniform spherical particles is 60%, and metallic particles with a density of 19 g/cm^3, 26 tonnes of fuel particles would occupy about 2,275 liters, or a height of 1.28 meters in a cylinder having diameter and height 1.5 meters – a bottom area of 1.77 m^2. The 5.4 m^3/s PRISM coolant flow through 1.77 m^2 would have an upward velocity of 3 m/s. As shown by Equation (2), uranium nitride particles smaller than 2.35 cm diameter would be carried out of the reaction region by this

[b] The AVR, built by Brown-Boveri-Krupp, was also partly controlled by the amount of fuel, which consisted of 6 cm balls in a stable bed [10, p. 7].

[c] This assumes that fuel in PRISM is fabricated with an initial 75% smear density, as in EBR-II [6].

[d] The density of liquid sodium at 633°K is 866.9 kg/m^3 [13].

velocity of coolant flow. To maintain a settled bed, particles as large as 20 cm diameter might be needed. Such large particles would be damaged by excessive thermal strain.

Allowing coolant to boil reduces the necessary flow rate. The energy W necessary to heat a liquid of mass m from temperature T_1 to T_2 at constant pressure, then boil it at T_2, then heat the vapor from T_2 to T_3 is

$$W = m \left[C_p^{\ell} (T_2 - T_1) + \Delta H_{\text{vap}} + C_p^{v} (T_3 - T_2) \right] . \quad (1)$$

Sodium enthalpy of vaporization ΔH_{vap} is 3,881 kJ/kg. Sodium vapor heat capacity C_p^v at 1,175°K is 2.53 kJ/kg/°K [13]. 840 MWth would be sufficient to heat 180 kilograms of sodium per second from 633°K to 1154.7°K, boil it, and heat the vapor to 1,200°K – about 0.21 kg s^{-1} MW^{-1}. At 633°K, the volume of 180 kilograms of liquid sodium is 207.6 liters.[d]

Metallic fuels as zirconium or molybdenum alloys would melt below the operating temperature. For example the solidus temperature of U-10Pu-30Zr (atomic percent) is below 1,200°K [14, P. 184]. Ceramic fuels or alloys containing beryllium or niobium are necessary. Beryllium has a much lower neutron absorption cross section. Nitride fuels would react less with sodium and structure than would carbide, oxide, or silicate fuels. Uranium-20% plutonium mononitride melts at 3,045±30°K [15]. A disadvantage of nitride fuels is that nitrogen-14 has a significant neutron absorption cross section, which decreases neutron economy and causes production of carbon-14. It would be necessary to use expensive nitrogen-15, which is only 0.366% of the atmosphere [16]. To the extent nitrogen is recovered when fuel is reprocessed [17], this cost is incurred only for the initial fuel load. The price of beryllium is about six times the price of uranium, but even with only 2 wt% beryllium, the fuel would melt above 1,800°K [7]. Beryllium undergoes the $^9\text{Be} \xrightarrow{(n,2n)} 2\alpha$ reaction, but it has a very small neutron absorption cross section, so it is mostly recovered during fuel processing; this cost is also therefore incurred only for the initial fuel load.

The uranium density observed in uranium nitride prepared by Johnson et al [18] was 13.55 g/cm^3. The overall density was 14.25 g/cm^3. Assuming 60% volume packing ratio for uniform spherical particles, the uranium volume fraction in a settled bed of uniform-size uranium nitride particles would be 57.1%.

Assuming simplistically that power density is linearly related to fuel volume fraction, and that the PRISM fuel volume fraction is the uranium volume fraction, the same power could be obtained with $28.3\%/57.1\% \times 26 \approx$ 12.9 tonnes of uranium, about 905 liters as nitride or 680 liters as 2 wt.% beryllium alloy. With nitride fuel and 60 vol.% fuel particles, the minimum sodium amount would be 600 liters, and the total volume would be about 1,500 liters. Assume for simplicity that the reaction region is a cylinder with diameter and height approximately 1.25 meters. The surface area of the bottom is 1.23 m^2. The vessel would be smaller with beryllium alloy fuel. Additional sodium in a taller vessel would ensure that fuel is always covered by sodium, even if working fluid flow to the heat exchanger is interrupted.

Coolant circulation in boiling homogeneous reactors is driven by coolant boiling. This conclusion was also reached in the context of aqueous homogeneous reactors [19, p. 145]. There are no pumps.

The density of sodium vapor at 1,200°K is 0.394 kg/m^3 [13]. Boiling 180 kilograms of sodium per second and heating it to 1,200°K would produce 180 / 0.394 = 456 m^3/s = 456,000 liters of sodium vapor per second.

Because the amount of circulating coolant is small, and the reaction volume is small, thermal inertia is small and power output can be changed rapidly.

In the present concept, the entire volume of sodium used for flowing coolant through fuel, about 2,000 liters, becomes contaminated with fission products and must be purified continuously. In PRISM, sodium in the 840 cubic meter (840,000 liter) pool is used as coolant [12]. Purifying that volume of sodium would be prohibitive, and the entire containment vessel, not only the reaction region, would become contaminated. The amount of sodium in an isolated circulating entirely-liquid sodium cooling system, a loop-within-pool design, would be less, but still large, and would require an additional heat exchanger and associated pumps.

The heat exchanger is shown schematically in Figure 2. After sodium is condensed to transfer its heat to the working fluid, it flows downward, around the outside of the reaction region, thence between the neutron reflector and sodium pool so as to remain a liquid, thence through the fuel to boil again. Although not shown in Figure 1, the top of the chimney would be convergent as shown in Figure 2 , with a neutron reflector below the heat exchanger.

The fluid that passes through the heat exchanger might be a transfer fluid, or the working fluid. If the fluid exits the heat exchanger at the same temperature as the entering sodium vapor, and if the fluid is sodium, it will enter the heat exchanger as a liquid and leave as a vapor. The heat exchanger is therefore not conceptually different from a steam generator in a more conventional system. Heckman proposed to use sodium vapor directly in a turbine [20] [10, p. 37, 46]. Rossbach and Wesling reported on a General Electric project, under contract to NASA, to build a 500 kw potassium vapor turbine for space nuclear applications, to evaluate materials compatibility [21]. Potassium has a lower boiling point than sodium, but the smaller enthalpy of vaporization and heat capacity would result in a greater coolant flow rate, as would also be the cause using rubidium or caesium, as shown in Table 1. Using lithium would allow a flow rate 39% the rate for sodium, but would require a much higher boiling point (1617.2°K). The alternative to boiling sodium in the heat exchanger is to use a sufficiently high working fluid flow rate, or a sufficiently high pressure, that it does not boil. This would reduce total plant thermal efficiency, require additional pumps and more robust structure, and increase plant cost. In the PRISM design, the rate is 5,400 liters per second [12]. In either case, the balance of plant could be similar to the PRISM design.

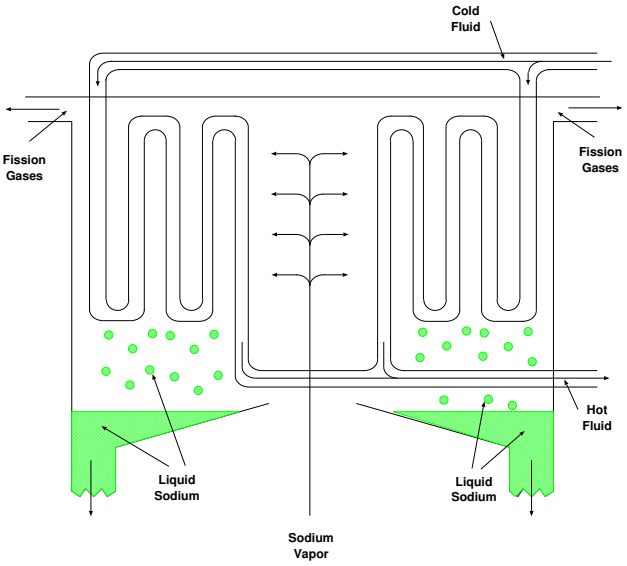

Figure 2: Heat Exchanger in More Detail

Table 1: Thermophysical Properties of Alkali Metals [22]

Metal	Lithium	Sodium	Potassium	Rubidium	Caesium
Boiling °K	1611.6	1154.7	1029.9	953.0	940.7
ΔH_{vap} kJ/kg	18239	3881	1959	802	494
Density kg/liter 600°K	0.5041	0.8732	0.7670	1.3397	1.6663
ΔH_{vap} kJ/liter	9160	3881	1567	1168	855.8
C_p liquid 600°K kJ/liter/°K	8.474	1.338	1.004	0.263	0.139
Flow rate, liter/MW	0.088	0.224	0.659	0.741	1.015
Saturation pressure bar at	1.771	0.5965	1.864	1.467	1.663
saturation temperature °K	1700	1200	1100	1000	1000

ΔH_{vap} for lithium from [23]. Saturation pressures from [24].

The sodium pool would be much smaller than in PRISM because most of the reaction heat is carried away by the separately-circulating and boiling coolant. Its primary purpose would be to buffer decay heat during shutdown. It would contain a heat exchanger of significantly less capacity than in the PRISM design. Coolant that returns from the plant's cooling tower would pass first through the pool heat exchanger before entering the chimney heat exchanger. A heat exchanger within the downward-flowing coolant, taking working fluid from the pool heat exchanger and delivering it to the chimney heat exchanger, might increase thermal efficiency.

3 Coolant Flow

Equating the drag force F_d on a particle to the force of gravity F_g determines the velocity U_t at which particles are suspended in equilibrium with upward fluid flow:

$$F_d = \frac{1}{2}\, C_d\, \rho_c\, U_t^2\, \pi\, \frac{d_f^2}{4} = F_g = \frac{4\pi}{3}\, \frac{d_f^3}{8}\, \rho_f\, g, \text{ or}$$
$$U_t = \sqrt{\frac{4\, g}{3\, C_d}\, \frac{\rho_f}{\rho_c}\, d_f}\,, \tag{2}$$

where

g = acceleration of gravity = 9.81 m/s^2,
d_f = fuel particle diameter, meters,
ρ_f = fuel particle density, see Table 2,
ρ_c = coolant density, see Table 2,
C_d = the Reynolds-number dependent drag coefficient (Kloosterman et al [25] used $C_d = 0.445$), and
U_t = upward coolant equilibrium terminal flow velocity, m/s.

Table 2: Coolant Densities ρ_c and Terminal Velocities U_t

	Coolant Density ρ_c kg/liter		Uranium Nitride $U_t\sqrt{d_f}$ m/s		U-2Be $U_t\sqrt{d_f}$ m/s	
Metal	Liquid	Vapor	Liquid	Vapor	Liquid	Vapor
Lithium	0.502	0.732×10^{-4}	28.88	2393	33.08	2741
Sodium	0.805	0.394×10^{-3}	22.81	1031	26.13	1181
Potassium	0.768	0.875×10^{-3}	23.36	692	26.76	793
Rubidium	1.382	0.165×10^{-2}	17.41	503	19.94	576
Caesium	1.679	0.298×10^{-2}	15.79	375	18.09	429

A 1.25 meter diameter reaction cylinder with a bottom cross section of 1.23 m^2 would be filled to a depth of about 1.25 meters by 1,500 liters of settled fuel paste. The upward velocity of 5.4 m^3/s of liquid sodium would be 4.4 m/s. The upward velocity of 207.6 liters per second of liquid sodium would be 0.167 m/s. The upward velocity of 456 m^3/s of sodium vapor would be 371 m/s. The speed of sound in sodium vapor at 1,200°K is 802 m/s,[e] so this is subsonic flow at Mach 0.46. Table 3 shows the relationship of particle sizes d_f to terminal velocity U_t.

Table 3: Particle sizes d_f

U_t	nitride	alloy
4.4 m/s liquid	3.72 cm	2.79 cm
0.167 m/s liquid	53.6 μm	40.8 μm
456 m/s vapor	19.6 cm	14.9 cm

The void fraction of particles ϵ_v, coolant flow velocity U, and the terminal velocity U_t, the velocity above which particles would be entrained in coolant and carried away, are related by the Richardson-Zaki relation [26]:

$$\epsilon_v = \left(\frac{U}{U_t}\right)^{\frac{1}{n}} \text{ or } U_t = U\, \epsilon_v^{-n}\,, \tag{3}$$

where the Richardson-Zaki constant $n \approx 2.4$, assuming the Reynolds number[f] is greater than about 500. The minimum possible void fraction with uniform-size particles is 0.4. Solving Equation (3) for U with $\epsilon_v = 0.4$ gives the velocity for a stable fuel bed $U_s = 0.111\, U_t$.

[e] The speed of sound is given by $v_s = \sqrt{\frac{C_p\, R\, T}{C_v\, M}}$ where $C_p = 1.279$ is the heat capacity of sodium vapor at constant pressure at 1200°K, $C_v = 0.862$ is the heat capacity of sodium vapor at constant volume at 1200°K [13, Table 1.1-5], R = 8.314 J/(mol K) is the gas constant, T = 1200 is temperature in kelvins, and M = 0.022989769 kg is the molar mass of sodium.

[f] The Reynolds number is $Re = \frac{\rho\, U\, D}{\mu}$. With $\rho = 743$ kg/m^3 at 1154°K, $U = 0.109$ m/s, $D = 1.5$ m, and $\mu = 1.49 \times 10^{-5}$ Pa·s, the Reynolds number for liquid sodium is about $Re = 8.15 \times 10^6$.

There are three possible regimes for fuel in the reaction region:

$U > U_t$ Fuel is entrained in coolant and carried out of the reaction region (this is called a *slurry reactor*). Slurry reactors were studied and rejected because of reactivity instability caused by slurry collapsing to a higher density settled bed if coolant flow ceases. With coolant flow caused by boiling rather than by pumps, its flow rate is proportional to power output, assuming the coolant does not all boil, and a slurry reactor might be feasible. Fuel entering the heat exchanger would contaminate it, and might damage it by abrasion. Fuel particles, except ones very much smaller than the design size, could be separated from vapor by a cyclone separator, which would reduce efficiency and move the abrasion problem from the heat exchanger to the much simpler separator.

$U_s < U < U_t$ Fuel is levitated but not carried out of the reaction region (this is called a *fluidized bed reactor*). Fluidized bed reactors have been described [11] [25], but not deployed commercially. In some designs, they would have the same reactivity instability as slurry reactors, but might also be feasible if coolant flow is caused by boiling. With a sufficiently tall chimney, only tiny fuel particles would enter the heat exchanger.

$U < U_s$ Coolant flows around fuel without significantly levitating it (this is called a *pebble bed reactor*). This would not have a reactivity instability caused by slurry or fluidized bed collapse. Gale Young reviewed the data on heat transfer and pressure drop in pebble piles cooled by gases, and concluded that they were likely to have poor performance [27] [10, p. 12]. AEC and Brown-Boveri-Krupp believed the problems were sufficiently solved and began construction of the 15 MWe AVR[g] reactor in 1959, which was in service in Jülich from 1969 until 1988. It suffered many accidents, earning the nickname "shipwreck." Pebble bed reactors were developed in South Africa, but not widely used.

The coolant velocity, and therefore the regime in which the reactor operates, is determined by the relationship of coolant flow rate to reaction region diameter. By equating $U_t = F/A$ to Equation (2), where F is coolant volumetric flow rate and A is the area through which it flows, the diameter d_r of the reaction region aperture for which the coolant velocity is U_t can be computed as a function of fuel particle diameter:

$$d_r = \sqrt[4]{12 \frac{F^2}{\pi^2} \frac{C_d}{g} \frac{\rho_c}{\rho_f d_f}} = \begin{array}{ll} \text{UN} & \text{U-2\%Be} \\ \frac{0.750}{\sqrt[4]{d_f}} & \frac{0.701}{\sqrt[4]{d_f}} \quad \text{(vapor at } F = \ 456 \text{ m}^3\text{/s)} \\ \frac{0.108}{\sqrt[4]{d_f}} & \frac{0.100}{\sqrt[4]{d_f}} \quad \text{(liquid at } F = \ 0.167 \text{ m}^3\text{/s), or} \\ \frac{0.549}{\sqrt[4]{d_f}} & \frac{0.513}{\sqrt[4]{d_f}} \quad \text{(liquid at } F = \ 5.4 \text{ m}^3\text{/s)}, \end{array} \tag{4}$$

where d_f is particle diameter in meters. Table 4 shows reaction region diameters for several diameters of particle and several vapor and liquid flow rates.

To reduce the velocity to $U_s = 0.111\, U_t$ without increasing particle size, it is necessary to increase d_r by a factor of $1/\sqrt{0.111} \approx 3$.

Table 4: Vessel Diameters d_r (meters) for $U = U_t$

	Flow rates m^3/s UN			Flow rates m^3/s U-2%Be		
d_f	456 vapor	0.167 liquid	5.4 liquid	456 vapor	0.167 liquid	5.4 liquid
10 nm	75.06	10.76	54.90	70.12	10.05	51.29
50 μm	8.93	1.28	6.53	8.34	1.20	6.10
100 μm	13.34	1.91	9.76	12.47	1.79	9.12
1 mm	4.22	0.61	3.09	3.94	0.57	2.88
1 cm	2.37	0.34	1.74	2.22	0.32	1.62

[g] Arbeitsgemeinschaft Versuchsreaktor or Working Group's Experimental Reactor

There is a tension between small particle size, coolant velocity, and vessel diameter. Smaller particle sizes result in more fission-product diffusion into sodium, thereby increasing burnup and reducing fuel processing cost, but require a larger vessel to avoid entraining fuel particles. If a slurry reactor remains stable with boiling coolant, the best particle size is the smallest one.[h]

For a stable bed in a cylindrical region, a "pancake" shape is required for small particles. Achieving criticality might not be possible except with a much larger fuel load per watt of output. A pancake would have poor neutron economy, and breeding would be much reduced. Alternatively, the vessel can have a concave shape, such as a hemisphere, cone ($d_r = 2\,h\tan\alpha$), paraboloid ($d_r = 2\sqrt{h/a}$), intermediate shape ($d_r = 2(h/a)^\alpha$, $1/2 < \alpha < 1$), or a divergent shape such as a hyperboloid, that might have better neutron economy, so that liquid entering at the bottom does not entrain (or levitate) particles, and vapor exiting at the top of the sodium above fuel does not entrain (or levitate) particles. Excess sodium above fuel, significantly beyond the 40% volume mixing ratio for a settled paste, would prevent all but the smallest fuel particles from being entrained into vapor.

Sefidvash proposed a conical vessel in a fluidized-bed reactor concept description [11].

Three-phase flow calculations, or experiments, would be necessary to choose an appropriate shape and particle size such that the fuel mixture remains stable and does not oscillate, and such that vapor escapes from fuel uniformly and does not "burp." These experiments could be done at small scale using various vessel shapes, induction heating, and depleted uranium nitride or U-2%Be.

4 Stability

4.1 For uranyl sulfate in water

Stein and Kasten [28] studied the fluid thermodynamics and neutron kinetics of boiling solutions of uranyl sulfate (UO_2SO_4) in heavy water. They concluded that the relationship between delayed neutron reactivity and void reactivity results in such reactors being inherently stable. At low rates of addition of reactivity (increasing the fuel concentration in the fluid mixture), power increased asymptotically to a stable value. At high rates power increased rapidly but only moderately above the desired stable value, and then declined asymptotically. In neither case were continuous oscillations observed.

To study hydraulic stability, Stein and Kasten computed the vapor fraction and enthalpy of vaporization at many temperatures, using data from [29] and the following method, the details of which are presented in [28]:

Volume of liquid:

$$V_l = \frac{m_t - \rho_g V_r}{\rho_l - \rho_g}\,, \tag{5}$$

where m_t is the total mass of liquid and vapor, ρ_g is the density of gas, V_r is the total volume of the reaction vessel, including both the liquid space and the vapor space above it, and ρ_ℓ is the density of liquid.

Volume of gas V_f within the reaction region:

$$V_f = \frac{m_t - V_l\rho_\ell - m_s}{\rho_g}\,, \tag{6}$$

where V_ℓ is the volume of liquid and m_s is the mass of gas in the heat exchanger.

Density:

$$\rho = \rho_\ell(1 - v_g) + \rho_g v_g\,, \tag{7}$$

[h] Small particles are less damaged by thermal strain, swell less, and more fission products diffuse to sodium.

where $v_g = V_f/V_\ell$ is the volume fraction of gas in the reaction region.

Enthalpy of vapor in the reaction region:

$$H = V_f \rho_g h_{fg}\,, \tag{8}$$

where h_{fg} is the specific enthalpy of vaporization.

From these data, the following correlation was obtained:

$$H = \frac{a}{\rho - b} - d = \frac{205.326 \times 10^6}{\rho - 21.1317} - 7.0598 \times 10^6 \text{ BTU per lb/ft}^3\,, \tag{9}$$

In the steady state, nuclear power production is directly proportional to the rate of heat removal from the reactor solution. Neglecting any change in the heat content of the liquid, if the heat extraction rate remains constant at P_0, the heat content of the vapor bubbles is time dependent upon the nuclear power.

Let

P_0 = power removal from reactor unit,
$\lambda(\epsilon)$ = normalized distributed bubble time delay function,
ϵ = time delay of bubble formation,
H = $V_f h_{fg} \rho_g$ = enthalpy of vapor in fluid, and
h_{fg} = enthalpy of vaporization (kJ/kg).

Then

$$\frac{\mathrm{d}H}{\mathrm{d}t} = \alpha \int_0^\infty \lambda(\epsilon)[P(t-\epsilon) - P_0]\,\mathrm{d}\epsilon = \alpha \int_0^\infty \lambda(\epsilon) P(t-\epsilon)\,\mathrm{d}\epsilon - \alpha\, P_0\,, \tag{10}$$

(the latter because $\int_0^\infty \lambda(\epsilon)\,\mathrm{d}\epsilon = 1$), where α is a units conversion factor, $\frac{3413}{3600}$ for BTU/kw-s, or 1 for SI units. Let B^2 be the so-called buckling factor, equal to $\left(\frac{\pi}{R}\right)^2$ for a sphere, and M^2 the migration area, approximated by $M^2 = M_0^2 \left(\frac{\rho_0}{\rho}\right)^2$, where ρ is reactor fluid density including vapor and ρ_0 is steady-state density.

For a cylindrical reactor

$$B^2 = \left(\frac{j_{0,1}}{R}\right)^2 + \left(\frac{\pi}{L}\right)^2 = \left(\frac{j_{0,1}}{R}\right)^2 + \left(\frac{\pi}{\gamma R}\right)^2\,, \tag{11}$$

where L is the height of the reactor, R is its radius, $\gamma = L/R$, and $j_{0,1} \approx 2.405$ is the first zero of $J_0(x)$, the Bessel function of the first kind and order zero [9, Eq. 7.20].

The critical multiplication constant is

$$k_c = 1 + B^2 M^2\,. \tag{12}$$

It is clear that for k_c to remain constant, $R\,\rho$ must remain constant.

Letting m be the mass of the reactor fluid, i.e., $\rho = m/V_r$, and with $V_r(0) = \pi R^2 L_0$, where L_0 is the steady-state height of the reactor fluid, differentiating Equation (12) with respect to ρ and using Equation (11) for the buckling factor yields

$$
\begin{aligned}
\frac{\mathrm{d}k_c}{\mathrm{d}\rho} &= B^2\frac{\mathrm{d}M^2}{\mathrm{d}\rho} + M^2\frac{\mathrm{d}B^2}{\mathrm{d}\rho} = -2\frac{M^2B^2}{\rho} + M^2\frac{\mathrm{d}B^2}{\mathrm{d}L}\frac{\mathrm{d}L}{\mathrm{d}\rho} \\
&= -2\frac{M^2}{\rho}\left[B^2 - \left(\frac{\pi}{L}\right)^2\right] = \frac{2}{\rho}\left[\frac{M^2\,B^2\left(\frac{j_{0,1}}{R}\right)^2}{\left(\frac{\pi}{L}\right)^2 + \left(\frac{j_{0,1}}{R}\right)^2}\right] \\
&= -2\frac{k_c-1}{\rho\left[1+\left(\frac{\pi R^3\rho}{j_{0,1}m}\right)^2\right]} = -2\frac{k_c-1}{\rho\left[1+\left(\frac{\rho}{\rho_0}\frac{\pi R}{j_{0,1}L_0}\right)^2\right]} = -2\frac{k_c-1}{\rho\left[1+\left(\frac{\rho}{\rho_0}\frac{\pi}{j_{0,1}\,\gamma}\right)^2\right]}\,.
\end{aligned}
\tag{13}
$$

Integrating Equation (13) with $k_c = k_{c0}$ when $\rho = \rho_0$ results in

$$
\frac{k_c-1}{k_{c0}-1} = \frac{\left(\frac{\rho_0}{\rho}\right)^2 + \left(\frac{\pi}{j_{0,1}\,\gamma}\right)^2}{1+\left(\frac{\pi}{j_{0,1}\,\gamma}\right)^2}\,,
\tag{14}
$$

It is still necessary to find the correspondence between multiplication constant, time, power, and vapor fraction of fluid v_g (or equivalently, fluid density ρ). From the two-group diffusion theory for one region thermal reactors, the time dependent equation for power as a function of k is (see, e.g., [9])

$$
\begin{aligned}
\frac{\mathrm{d}P(t)}{\mathrm{d}t} &= -\lambda_0\left[(\beta-1)k(t) + k_c(t)\right]P(t) + \sum_i \lambda_i\mu_i(t) \\
\frac{\mathrm{d}\mu_i(t)}{\mathrm{d}t} &= -\lambda_i\mu_i(t) + \beta_i k(t)\lambda_0 P(t)\,,
\end{aligned}
\tag{15}
$$

where

β $= \sum_i \beta_i$ = fraction of neutrons that result from fission product decay
β_i = fraction of neutrons having decay characteristic λ_i
λ_0 = reciprocal lifetime of prompt neutrons
λ_i = reciprocal lifetime of i^{th} delayed neutron emitter
μ_i = concentration of i^{th} delayed neutron emitter
k = material multiplication constant if finite pile has no leakage
k_c = multiplication constant required for criticality if finite pile has no leakage
P = power dissipation
t = time

Equations (9), (10), (14), and (15) mathematically describe the problem at hand. Using methods available at the time, it was necesary to simplify them. Stein and Kasten replaced Equation (15) with

$$
\frac{\mathrm{d}P(t)}{\mathrm{d}t} = \lambda_0[(1-\beta)k(t) - k_c(t)]P(t) + \lambda_0\,\beta\,k_{c0}\,P_0
\tag{16}
$$

and did not use equations for $\mu_i(t)$, for delayed neutrons.

In Equation (10) the form of the normalized distributed time delay function $\lambda(\epsilon)$ is unknown. Further, using Equation (10) results in a delay-integro-differential equation system. As a first approximation, let the vapor generated at time t result from nuclear power at time $t-\tau$, where τ is some discrete value. This corresponds to assuming that $\lambda(\epsilon) = \delta(\tau)$. Under this assumption, Equations (9) and (10) combine to yield

$$\frac{\mathrm{d}H(t)}{\mathrm{d}t} = \frac{\mathrm{d}\frac{a}{\rho(t)-b}}{\mathrm{d}t} = \alpha(P(t-\tau)-P_0) \text{ or } \frac{\mathrm{d}\rho(t)}{\mathrm{d}t} = \frac{\alpha}{a}(\rho(t)-b)^2(P(t-\tau)-P_0)), \tag{17}$$

This is still a delay-differential equation. For small τ and small $\frac{\mathrm{d}P}{\mathrm{d}t}$, approximate $P(t-\tau)$ by a first-order Taylor expansion. Equation (17) becomes

$$\frac{\mathrm{d}\rho(t)}{\mathrm{d}t} = -\frac{\alpha}{a}(\rho(t)-b)^2\left(P(t)-\tau\frac{\mathrm{d}P(t)}{\mathrm{d}t}-P_0\right). \tag{18}$$

Stein and Kasten speculated that using a probability density function other than $\lambda(\epsilon) = \delta(\tau)$ would produce more realistic results. But if one replaces $P(t-\epsilon)$ with a first-order expansion as in Equation (18), Equation (10) becomes

$$\frac{\mathrm{d}\rho(t)}{\mathrm{d}t} = -\frac{\alpha}{a}(\rho(t)-b)^2\left(P(t)-\frac{\mathrm{d}P(t)}{\mathrm{d}t}\int_0^\infty \epsilon\,\lambda(\epsilon)\,\mathrm{d}\epsilon - P_0\right). \tag{19}$$

The integral here is, however, a constant that depends only upon the choice of the distribution $\lambda(\epsilon)$ and its parameters, for example mean and standard deviation in a log-normal distribution. So Equations (18) and (19) are equivalent.

Collecting the equations we have

$$\begin{aligned}
k_c(t) &= 1 + (k_{c0}-1)\frac{\left(\frac{\rho_0}{\rho(t)}\right)^2 + \left(\frac{\pi}{j_{0,1}\,\gamma}\right)^2}{1+\left(\frac{\pi}{j_{0,1}\,\gamma}\right)^2} \\
\frac{\mathrm{d}\rho(t)}{\mathrm{d}t} &= -\frac{\alpha}{a}(\rho(t)-b)^2\left(P(t)-\tau\frac{\mathrm{d}P(t)}{\mathrm{d}t}-P_0\right) \\
\frac{\mathrm{d}P(t)}{\mathrm{d}t} &= -\lambda_0\left[(\beta-1)k(t)+k_c(t)\right]P(t) + \sum_i \lambda_i\mu_i(t)\ , \text{ or} \\
\frac{\mathrm{d}P(t)}{\mathrm{d}t} &= -\lambda_0\left[(\beta-1)k(t)+k_c(t)\right]P(t) + \lambda_0 k_{c0}P(0)\beta \ \text{ for } t < 0.1 \\
\frac{\mathrm{d}\mu_i(t)}{\mathrm{d}t} &= -\lambda_i\mu_i(t) + \lambda_0\beta_i k(t)P(t) \\
k(t) &= k_{c0} + \Delta k + Ct \text{ for several values of } \Delta k \text{ and } C\,,
\end{aligned} \tag{20}$$

where (using imperial units)

$k_{c0} = 1.06$
$\rho_0 = 44.91$ lb/ft^3
$j_{0,1} \approx 2.405$
$\gamma = 2$
$\alpha = \frac{3413}{3600}$ BTU/kw-sec
$a = 205.326 \times 10^6$
$b = 21.1317$
$\tau = [0 \ldots 0.003$ seconds$]$
$P_0 = 10^6$ kw
$\lambda_0 = 10^4$ sec^{-1}
$\beta_i = \{\ 0.00025,\ 0.00085,\ 0.00241,\ 0.00213,\ 0.00166,\ 0.00025\ \}$
$\lambda_i = \{\ 13.86,\ 1.61,\ 0.456,\ 0.154,\ 0.0315,\ 0.0215\ \}$ sec^{-1}
$\beta = \sum_i \beta_i = 0.00755$
$C = [0 \ldots 0.002215$/sec$]$.

Modern computers and numerical methods to solve differential equations were not available in 1951. Stein and Kasten used graphical methods, and considered several cases:

Case I $\beta = 0$, $\tau = 0$. This disregards delayed neutrons and delayed bubble formation time. The three subcases considered were with reactivity changed (1) instantaneously, (2) linearly with time, and (3) a combination of (1) and (2).

Case IA $k = k_{c0} + Ct$, increase of solution reactivity with time. This resulted in maximum P/P_0 about 2.155 after 0.384 seconds, oscillations with a period of about 0.77 seconds, and density variations oscillating with the same period and monotone decline in amplitude.

Caae IB $k = k_{c0} + 0.01 + Ct$, instananeous reactivity increase with and without increase with time ($C \neq 0$ and $C = 0$). Power increased by a factor of about 125 within 0.0612 seconds, returning to about 1.0 within about 0.15 seconds, and a total period of about 3.25 seconds with C = 0.002215/sec and about 4.8 seconds with C = 0. Very rapid and significant density changes occurred.

Case IC $k = k_{c0} + 0.02$, as in Case IB with $C = 0$, instantaneous reactivity increase only. This resulted in maximum P/P_0 in about 0.038 seconds and oscillations with a period of about 9.3 seconds, and more extreme density variations.

Such oscillations are undesirable, but are unrealistic because the damping effects of delayed neutron emission and bubble formation are ignored.

Case II $\beta = 0.005$, $\tau = 0$, $C = 0.002215$. This case considers the effect of delayed neutrons but not the effect of delayed bubble formation.

Case IIA $k = k_{c0} + Ct$. No power oscillations, rather a slow rise in power approaching an equilibrium P/P_0 value about 1.5.

Case IIB $k = k_{c0} + 0.00177 + Ct$. Maximum P/P_0 slightly greater than 1.5, decreasing rapidly to equilibrium about 1.5.

Case IIC $k = k_{c0} + 0.0053 + Ct$. Maximum P/P_0 is about 4.8, decreasing to P/P_0 value about 1.5 within about two seconds.

Density decreased uniformly in all cases. This illustrates the damping effect of delayed neutrons on the effect of reactivity increases.

Case III $\beta = 0$, $\tau = \{0.004, 0.01\}$ seconds, $C = 0.002215$.

These cases consider the effect of delayed bubble formation but not the effect of delayed neutrons. As in Case I, These cases result in oscillations, with the magnitude diverging. Divergence is not rapid, but increases with increasing τ.

Case IV $\beta = 0.00406$, $\tau = 0.01$, $C = 0.002215$.

Case IVA $k = k_{c0} + 0.0043036$, instantaneous addition of reactivity. The positive damping action of delayed neutrons completely overshadows the negative damping of bubble formation. Maximum P/P_0 about 4.4 within about 0.1 seconds, reducing to equilibrium in about one second.

Case IVB $k = k_{c0} + 0.0043036 + Ct$. Similar to Case IVA, but with maximum P/P_0 of about 5.4 after about 0.15 seconds, and slower reduction to equilibrium.

Case IVC $k = k_{c0} + 0.0043036 + Ct$ and a delayed neutron group with $\lambda_i = 0.154$. One delayed neutron group helps maintain the power level but the overall effect is small.

Case IVD $k = k_{c0} + 0.0088$. Maximum P/P_0 about 48.

Stein and Kasten concluded that the effect of delayed neutrons entirely overshadows the effect of bubble delay times up to 0.01 seconds for instantaneous reactivity increases Δk of 0.009, which they considered to be extreme. If τ is large, only small values of Δk can be tolerated, but large power pulses result in smaller values of τ and small power pulses result in large values of τ. They recommended that $\lambda(\epsilon)$ in Equation (10) should be considered to be a distributed time delay function, not a delta function – but see the discussion following Equation (19).

4.2 Correlation between H and ρ for water and sodium

Using equations from [13] for sodium density (page 86) and enthalpy of vaporization (page 65), and for water from [30], the same procedure that was used by Stein and Kasten was undertaken for sodium, to relate H to ρ as in Equation (17), and for the same purpose for sodium using modern numerical methods. Adding an exponent to be solved for in the denominator, the correlation obtained for water was

$$H = V_f \rho_g h_{fg} = \frac{a}{(\rho - b)^c} - d = \frac{7.339655 \times 10^9}{(\rho - 330.239)^{1.14616}} - 6.187961 \times 10^6 \tag{21}$$

in SI units. The standard deviation of the relative error for the fit was 2.694×10^{-4}.

The correlation obtained for sodium was

$$H = V_f \rho_g h_{fg} = \frac{a}{(\rho - b)^c} - d = \frac{358477}{(\rho - 389.189)^{0.951695}} - 1346.07 \tag{22}$$

in SI units. The standard deviation of the relative error for the fit was 2.038×10^{-4}.

4.3 Solutions using modern numerical methods

Let $\sigma(t) = \frac{P(t)}{P_0}$, $\phi(t) = \frac{\rho(t)}{\rho_0}$, and $\zeta_i(t) = \frac{\mu_i(t)}{\mu_i(0)}$. This normalization allows to use the same error tolerance while integrating all of these differential equations, assuming deviation from initial conditions is less than an order of magnitude. Then

$$\begin{aligned}
k_c(t) &= 1 + (k_{c0} - 1) \frac{\left(\frac{1}{\phi(t)}\right)^2 + \left(\frac{\pi}{j_{0,1}\,\gamma}\right)^2}{1 + \left(\frac{\pi}{j_{0,1}\,\gamma}\right)^2}\,, \\
\frac{\mathrm{d}\phi(t)}{\mathrm{d}t} &= -\frac{\alpha \rho(0)^c P(0)}{ac} \left(\phi(t) - \frac{b}{\rho(0)}\right)^{c+1} \left(\sigma(t) - \tau \frac{\mathrm{d}\sigma(t)}{\mathrm{d}t} - 1\right)\,, \\
\frac{\mathrm{d}\sigma(t)}{\mathrm{d}t} &= -\lambda_0 \left[(\beta - 1)k(t) + k_c(t)\right] \sigma(t) + \frac{1}{P(0)} \sum_i \lambda_i \mu_i(0) \zeta_i(t)\,, \text{ or,} \\
\frac{\mathrm{d}\sigma(t)}{\mathrm{d}t} &= -\lambda_0 \left[(\beta - 1)k(t) + k_c(t)\right] \sigma(t) + \lambda_0 k_{c0} \beta \text{ if } \zeta_i \text{ equations are not used}\,, \\
\frac{\mathrm{d}\zeta_i(t)}{\mathrm{d}t} &= -\lambda_i \zeta_i(t) + \frac{\lambda_0 \beta_i P_0}{\mu_i(0)} k(t) \sigma(t)\,, \\
k(t) &= k_{c0} + \Delta k + Ct \text{ for several values of } \Delta k \text{ and } C\,.
\end{aligned} \tag{23}$$

Using a first-order Taylor expansion was found not to be adequate so a second-order expansion was used. Equation (19) becomes

$$\frac{\mathrm{d}\rho(t)}{\mathrm{d}t} = -\frac{\alpha}{a}(\rho(t) - b)^2 \left(P(t) - \frac{\mathrm{d}P(t)}{\mathrm{d}t} \int_0^\infty \epsilon\, \lambda(\epsilon)\, \mathrm{d}\epsilon + \frac{\mathrm{d}^2 P(t)}{\mathrm{d}t^2} \int_0^\infty \frac{\epsilon^2}{2}\, \lambda(\epsilon)\, \mathrm{d}\epsilon - P_0\right)\,. \tag{24}$$

Replacing the integrals in Equation (24) with τ and $\tau^2/2$ is not precisely correct because the first moment of a distribution is not generally equal to its second moment, unless $\lambda(\epsilon) = \delta(\tau)$. This assumption was nonetheless found to result in more stable computations than using a first-order Taylor expansion.

Using the second-order Taylor expansion required to add

$$\frac{\mathrm{d}^2\sigma(t)}{\mathrm{d}t^2} = -\lambda_0\left[(\beta-1)k(t)+k_c(t)\right]\frac{\mathrm{d}\sigma(t)}{\mathrm{d}t} - \lambda_0\left[(\beta-1)\frac{\mathrm{d}k(t)}{\mathrm{d}t}+\frac{\mathrm{d}k_c(t)}{\mathrm{d}t}\right]\sigma(t)+ \frac{1}{P(0)}\sum_i \lambda_i\mu_i(0)\frac{\mathrm{d}\zeta_i(t)}{\mathrm{d}t}\,. \tag{25}$$

$\frac{\mathrm{d}^2\sigma(t)}{\mathrm{d}t^2}$ depends upon $\frac{\mathrm{d}k_c(t)}{\mathrm{d}t}$, which in turn depends upon $\frac{\mathrm{d}\phi(t)}{\mathrm{d}t}$. Let

$$\frac{\mathrm{d}\phi(t)}{\mathrm{d}t} = -R\left(\sigma(t)-\tau\frac{\mathrm{d}\sigma(t)}{\mathrm{d}t}+\frac{\tau^2}{2}\frac{\mathrm{d}^2\sigma(t)}{\mathrm{d}t^2}-1\right), \tag{26}$$

where

$$R = \frac{\alpha\rho(0)^c P(0)}{ac}\left(\phi(t)+\frac{b}{\rho(0)}\right)^{c+1}. \tag{27}$$

After solving, we have

$$\frac{\mathrm{d}\phi(t)}{\mathrm{d}t} = -R\left(1+\frac{R\tau^2\lambda_0(k_{c0}-1)\sigma(t)}{\phi(t)^3\left(1+\left(\frac{\pi}{j_{0,1}\gamma}\right)^2\right)}\right)^{-1} \left(\sigma(t)-\tau\frac{\mathrm{d}\sigma(t)}{\mathrm{d}t}-1 +\frac{\tau^2}{2}\left(-\lambda_0[(\beta-1)k(t)+k_c(t)]\frac{\mathrm{d}\sigma(t)}{\mathrm{d}t}+\sum_i\frac{\lambda_i\mu_i(0)}{P(0)}\frac{\mathrm{d}\zeta_i(t)}{\mathrm{d}t}\right)\right). \tag{28}$$

For water, the values of P_0 and ρ_0 from Stein and Kasten, and $c = 1$, were used, converted to SI units. For sodium, the same value of P_0 was used, but $\rho_0 = 669.34$ kg/m^3. In both cases, $\mu_i(0) = \lambda_0\beta_i(k_{c0}+\Delta k)P_0/\lambda_i$.

Equations (23) are stiff, so the differential equation solver LSODE from ODEPACK [31] was used, with $\sigma(0) = \phi(0) = \zeta_i(0) = 1$. The local error tolerance was 10^{-11}. The step size was less than one millisecond. Modern values of λ_0, λ_i, and β_i were taken from [9, p. 123]. Results that were rather different from those obtained by Stein and Kasten were obtained for both water and sodium.

With $k_c = 1.06$ and $\Delta k = 0$, small but rapid oscillations initially appeared, but damped out within a few seconds. Thereafter, σ, ρ, and ζ_i all stabilized at values slightly greater than 1.0. Equations (23) are very sensitive to the value of k. Solving with $\Delta k = 0.0011142$, or equivalently with $k_{c0} = 1.0611142$ instead of 1.06, resulted in equilibrium values very close to 1.0.

As shown in Figure 3, with these values for Δk or k_{c0}, for water with $\tau = 0$ or 0.00365, P/P_0 initially increased to 1.06 and ρ/ρ_0 increased to 1.2. After about 100 seconds, P/P_0 decreased to 0.99 and ρ/ρ_0 decreased to 0.99. After 150 seconds, both P/P_0 and ρ/ρ_0 were stable at 1.0. Delayed neutrons increased for about 50 seconds, but all ζ_i stabilized at about $1.2\,\zeta_i(0)$ after about 300 seconds. The behavior with $\tau = 0$ and $\tau = 0.00365$ was almost exactly the same.

For sodium with $\tau = 0$, P/P_0 initially increased to $(1 + 3\times10^{-6})$ but stabilized at $P = P_0$ within 0.03 seconds. ρ/ρ_0 decreased within 0.03 seconds and stabilized at $(1 - 1.45\times10^{-5})$. The only differences with $\tau = 0.00365$ were that P/P_0 initially increased to $(1+4\times10^{-6})$, and ρ/ρ_0 decreased to $(1-1.6\times10^{-5})$ before stabilizing at the same values as for $\tau = 0$. Delayed neutrons stabilized with $\zeta_i = 1$ within five seconds. If the method of Stein and Kastan is applicable to the present concept, the results in Figure 3 suggest remarkable stability if reactivity is not added continuously, i.e., if $C = 0$.

With those starting values for Δk or k_{c0}, oscillations other than the single initial brief starting oscillation were not observed for either sodium or water. All calculations were started with $\sigma(0) = \rho(0) = \zeta_i(0) = 1$, so they were simulations of what were expected to be steady-state conditions. Starting with $\sigma(0) = 0.5$ produced very similar results, with the initial single oscillation lasting somewhat longer. When started at the expected steady-state conditions, the initial oscillations were most likely numerical, not physical, in nature. The conclusion is that the negative reactivity effect of delayed neutrons overwhelms the positive reactivity effect of immediate bubble formation, resulting in a boiling reactor fueled with an aqueous solution of uranyl sulfate, or fueled with finely-divided particles of uranium metal (^{235}U and ^{238}U) in sodium, being stable.

These are of course, only mathematical studies, but the results obtained by Stein and Kasten were qualitatively verified by experiments using the SUPO reactor [32] [33, pp. 133ff]. This suggests that the system proposed here would also be inherently stable. More complete analyses, using the fuels and coolants proposed here, and small-scale experiments, should be undertaken to verify this hypothesis.

Metallic fuels are not soluble in sodium, so using Equations (23) for sodium assumes that fuel is uniformly distributed throughout the fluid.

As shown in Figure 4, for large values of τ, power and density increased over an interval of several minutes, after which both power and density decreased, primarily because density decreased significantly, that is, most of the sodium boiled. For small values of τ, power and density at first increased gradually. After about three minutes, power increased enormously by 26 orders of magnitude and then decreased almost as quickly, which resulted in an immediate decrease in density and an accompanying decrease in power.

5 Prior related art

More similar to the system proposed here than the system studied by Stein and Kasten [28], Petrick and Marchaterre [34] proposed a slurry reactor containing a boiling mixture of heavy water, $UO_3 \cdot H_2O$, and ThO_2, shown in Figure 5, which is taken from their patent [35]. They proposed the following advantages of a boiling water slurry reactor:

1. High specific power and high power density with small total fuel inventory.
2. High neutron economy because of the absence of structural elements and fuel cladding within the core, and the continuous removal of fission product neutron poisons.
3. Clean hydrodynamics, also because of the absence of structural elements within the core.
4. Continuous fuel processing.
5. Elimination of costly fuel fabrication methods.
6. Breeding potential, either within the core or in a blanket.
7. Excellent heat transfer characteristics.
8. Elimination of external fuel circulation, external heat exchangers, associated pumps, and associated remote maintenance systems because steam is drawn directly from the reaction region.
9. Excellent safety characteristics due to an exceptionally strong negative void coefficient.
10. Simplicity of operation and control without the use of mechanical control rods. Rapid power changes would be achieved by varying either core vapor

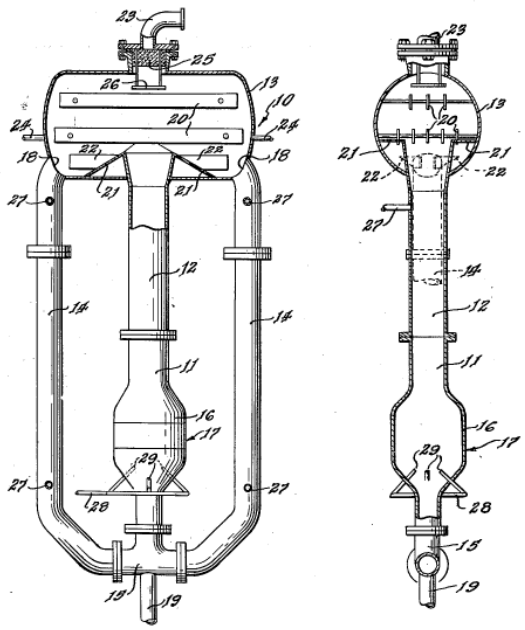

Figure 5: Boiling Slurry Reactor from Patent 3,088,895

fraction or circulation velocity. Slower power changes would be achieved by changing the enrichment or concentration of fuel.

11. Primary circulation is achieved by natural convection, not by pumps. Self agitation resulting from boiling would aid in maintaining uniform distribution of particles and reducing settling.

Petrick and Marchaterre were concerned about corrosion because the pH would need to be reduced by adding sulfuric acid, to prevent fuel particle caking or reduction of oxide to metal. They were also concerned about radiologic separation of hydrogen (or deuterium) and oxygen from coolant, and the need for methods to prevent them from recombining explosively. The successor study addressed a concern about valence change of urania [36, p. 44]. Those problems are not relevant to the present proposal.

Rather than steam arising from the top of a fuel mixture at the bottom of a vessel, they envisioned that the reactor contained sufficient water to fill the entire volume below the steam drum (object 13 in Figure 5). Steam would be separated somewhat during coolant rising through the riser sections of the reactor (objects 11 and 12), and then primarily within the steam drum. Therefore, coolant was circulating primarily as a liquid, not remaining within the reaction region as a liquid and circulating first as a vapor and then as a condensed liquid. A similar scheme could be used in the presently proposed system, but this would increase the amount of sodium needing to be purified continuously.

Circulation was maintained by the difference in density between fluid in the riser and downcomer sections of the reactor (objects 12 and 14).

The reaction takes place in a volume with a shape chosen to maintain criticality (objects 16 and 17). The riser and downcomer sections are narrower to create regions where criticality could not be maintained.

The primary mechanism of control was adjustment of circulation velocity. From [34, § IV]:

> Adjusting the recirculation velocity would cause the reactor power level to respond very quickly, since the reactor power will adjust to maintain the same amount of reactivity tied up in voids. A sudden increase in the recirculation velocity would produce a supercritical condition ($k_{\text{eff}} > 1$), since the core mean steam volume fraction would be lowered. The reactor power would therefore increase to again reestablish a just-critical system ($k_{\text{eff}} = 1$). A sudden drop in recirculation flow rate would automatically drop the reactor power level, since a subcritical system would tend to exist. The reactor can be controlled by velocity adjustment very quickly over wide ranges of power levels.

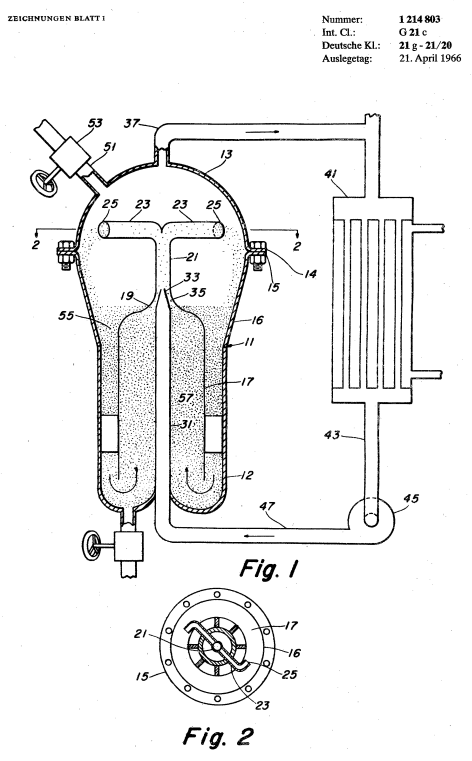

Figure 6: Slurry Reactor from German Patent 1,214,803

The method to control coolant circulation velocity was by changing the density relationship between the riser and downcomer legs by injecting gas into orifices at the top of the downcomer legs (objects 27), which would tend to slow circulation by reducing downcomer density, or at the bottom, which would tend to increase circulation by reducing reaction region and riser density. The void fraction was to be changed by injecting gas through orifices (objects 29) within the reaction region, which would decrease riser density and therefore increase circulation velocity. The gas to be used consisted of fission gases and an unspecified diluent (probably argon). Some

fission gases or fission product decay gases have thermal neutron absorption cross sections as much as 5.2 million times larger than sodium, but their atomic fraction within the system would be small. It would be necessary to remove them from the reactor and store them, at least long enough for ^{135}Xe to decay.

The proposed system would have operated at 250°C and 500 PSI. The thermal efficiency would have been quite low.

Petrick and Marchaterre did not propose that dumping slurry could be used as a safety system. A successor report for a more complete design for the experiment proposed by them included a storage coil with sufficient capacity for all water and oxide, active circulation, and a shape that did not allow criticality. They explicitly rejected gravity drain [36].

In German patent number 1,214,803, Harold McNeal Busey described a reactor containing a slurry of sodium and UO_2 particles, shown in Figure 6 [37]. Slurry is circulated within the reactor by an eductor pump (items 33 and 35). Sodium and fuel are separated by centrifugal action at the outlet of the eductor pump, as shown at the bottom of Figure 6 – similar in action to a hydroclone. Busey did not specify the operating temperature or quantify flow rates, did not explain how fuel would remain suspended if coolant circulation stopped or the effect of fuel settling in that event, did not propose that sodium would boil, but did remark that using fuel in intimate contact with sodium had the same effect of partial fuel processing described in Section 6.

Rymarz studied stability of UO_2-NaK slurries at temperatures up to 600°C, and concluded that flocculation did not occur [38]. Although the results might be relevant to nitride fuel, metallic fuel was not studied, and such studies should be undertaken.

6 Processing sodium and fuel

As shown in Figure 1, a small amount of fuel slurry is continuously removed for processing from the bottom of the connection between the reaction and storage regions, by an eductor powered by coolant sodium. Circulating and processing fuel and coolant, even during shutdown, continuously removes ^{135}I, the precursor to the powerful neutron poison ^{135}Xe, thereby reducing or eliminating the "iodine pit" startup control instability.

Alkali metal, alkaline earth, antimony, arsenic, cadmium, gallium, germanium, indium, sodium iodide, small amounts of tellurium, and tin fission products are soluble in sodium at operating temperatures. Nitride ceramics, actinides, lanthanides, noble metals, and inert gases do not dissolve in or react with sodium. Beryllium is almost insoluble in sodium [7]. Gases and sodium-soluble fission products, especially those that are not soluble in uranium, diffuse from fuel particles into sodium. Metals that have boiling points below 1154.7°K can be removed from coolant by condensing from vapor. Fragments that result from fission near fuel particle surfaces escape directly into coolant, but noble metals, lanthanides, and fuel are not dissolved. It would be necessary to separate them by hydroclones. Sodium-soluble fission product metals that have boiling points above 1154.7°K generally have melting points below sodium's boiling point, and can therefore be separated from liquid sodium by a cold trap. Temperatures higher than the sodium operating temperature would be needed to distill fission products that have boiling points higher than 1,154°K, e.g., to separate strontium (1655°K) from barium (2170°K).

Sodium and fuel are processed as described in [4]. Purified or replacement fuel is returned to the reaction region as a dilute slurry. To summarize:

1. Separate sodium from particles.
2. Return insufficiently consumed fuel particles to the reaction vessel, if it is possible to distinguish them, e.g., by density or photometry.
3. Distill sodium to purify it and separate sodium-soluble fission products. Argonne National Laboratory West (now Idaho National Laboratory) evaluated using distillation to purify sodium [39].
4. Remove fission products that have not diffused into sodium from sufficiently consumed fuel particles using the pyroelectric process developed for the Experimental Breeder Reactor II (EBR-II) [40].
5. Create particles from purified or replacement fuel.

A reactor of the same power as the 840 MWth PRISM reactor described above would produce about 956 grams of fission products per day. Sodium-soluble fission products constitute 12.2 wt.%, or 116 grams per day. With 2,000 liters of liquid sodium in the reaction vessel, the rate of increase of their concentration in circulating liquid coolant is less than 0.07 wt.% per day. Fission product gases constitute 16.4 wt.%, or 157 grams per day. Other fission products amount to 690 grams per day.[i]

Purify sodium continuously to remove sodium-soluble fission products from 2,000 liters = 1,464 kg of liquid sodium per day. As vapor at 1,200°K, 1,464 kilograms of sodium would occupy about 3,700 cubic meters. Withdrawing 0.043 m^3/s, or about 0.01% of the sodium vapor flow, and passing it through a distillation column, would remove caesium (943.3°K), selenium (957.6°K), and rubidium (961.2°K). A cold trap can remove tellurium (melting point 934.2°K), sodium iodide (934.2°K), barium (1,000°K), and strontium (1,050°K) from sodium separated from fuel slurry sent to processing. Alternatively, sodium separated from the reprocessing slurry can be heated by vapor, further heated to boil more of the fission products, and then passed through a distillation column. Cadmium should be continuously removed because ^{113}Cd has a significant neutron absorption cross section. Cadmium might, however, be difficult to remove by a cold trap (boiling point 1,040°K, melting point 594°K). If not removed, cadmium would accumulate at the rate of 1.43 kg/GWe-yr, but the only isotope with a significant neutron absorption cross section, ^{113}Cd, and the only significantly radiotoxic isotope, ^{113m}Cd (which has a half life of 14.10 years), are produced at the rate of 5.7 grams per GWe-yr [41]. Cadmium might damage fuel particles by forming low melting point alloys, decreasing the fraction of particles that can be returned without processing. Additional sodium-soluble fission products are produced in only millimole quantities per GWe-yr. Processing about 13.2 kg, about one liter of nitride particles, per day, about 4.8 tonnes per year, would maintain 5 wt.% concentration of fission products [42].

Even though sodium-soluble fission products diffuse from fuel into sodium, some remain within fuel particles. In "high" but unspecified burnup solid metallic fuel slugs from EBR-II, only 70% of alkali-metal fission products and 20% of alkaline earth fission products were found in bond sodium [6]. With smaller particles, more sodium-soluble fission products would be found in sodium. Caesium and strontium, the two fission products that produce 99.4% of radiotoxicity but constitute only 9.26 wt.% of fission products, are sodium soluble. It would be desirable to remove them before pyroelectric processing, to avoid incorporating them into the ceramic waste form [43]. Till and Chang wrote [40, p. 241] that removing them would "increase repository space utilization by the huge factor of 225.... In the absence of these two activities... there would simply be no need for a highly engineered repository."

One way to remove fission products that have not (but could have) diffused into sodium is to distill fuel as described in [4]. All fuel and fission product metals form hydrides, which decompose at various modest temperatures. For example, formation and decomposition of uranium hydride are in equilibrium at 225°C [44], and cadmium hydride decomposes at -20°C. As hydrides form and decompose, fuel particles are reformed with different distributions of fuel and fission products. If the hydride-dehydride process is carried out in or above sodium, it gives more opportunities for soluble fission products to dissolve into sodium rather than to be incorporated into fuel particles. Sodium-soluble fission products can then be separated from fuel particles by filtering and washing with clean sodium, or by a sequence of centrifugal contactors with a countercurrent flow of clean sodium. To the extent that particles re-formed after dehydriding are relatively pure, it might be possible to separate them according to density: The densities of most fission products are 30-50% of the densities of actinides. High-density particles can probably be returned to the reactor without further processing. The much smaller quantity of low-density particles could be processed pyroelectrically to remove residual actinides.

Oxidation of fuel particles at the anode in a pyroelectric processor is necessarily a surface phenomenon. Therefore, the larger surface-to-volume ratio of small particles, as compared to solid slugs, allows pyroelectric processing to proceed more rapidly.

[i] Output from the ORIGEN 2 computer program [41].

7 Inherent safety

The first line of defense against damage or injury is, of course, the active control system, and its human operators who continuously monitor temperatures, pressures, and flow rates, and adjust pressures above the reaction and storage regions or adjust power to electromagnetic pumps that lift fuel from the storage region to the reaction region.

Fuel, coolant, and structure expansion as temperature increased contributed to inherent passive safety in EBR-II [40]. That mechanism would be operative but less effective in the concept proposed here. Very high thermal conductivity of metallic fuel, very high thermal conductivity of sodium coolant, and very large heat capacity of the sodium pool were more important [45]. Those mechanisms would be at work here. Indeed, the thermal conductivity of paste or slurry is greater than the thermal conductivity of solid metal because the thermal conductivity of sodium ($\kappa_{\mathrm{Na}} \simeq 62.9$ $\mathrm{Wm^{-1}{}^{\circ}K^{-1}}$ [13, p. 101]) is greater than the thermal conductivity of uranium ($\kappa_f \simeq 35$ $\mathrm{Wm^{-1}{}^{\circ}K^{-1}}$ [46]).

The thermal conductivity of uranium nitride is less than metal, but still quite large. Ross developed the correlation $\kappa_f = 1.37\,T^{0.41}$ $\mathrm{Wm^{-1}{}^{\circ}K^{-1}}$ [47]. The thermal conductivity of paste fuel, $\kappa_p \approx 34.3$ $\mathrm{Wm^{-1}{}^{\circ}K^{-1}}$ at 630°K and $\kappa_p \approx 38.4$ $\mathrm{Wm^{-1}{}^{\circ}K^{-1}}$ at 1200°K, was estimated using Equation (6.4) from [48]:

$$\frac{\kappa_p}{\kappa_{Na}} = 1 + 3\beta\phi + 3\beta^2\phi^2\left(1 + \frac{9\beta}{16(\beta+5)} + \frac{\beta}{4} + \frac{\beta^2}{2^6} + \dots\right) + O(\phi^3)\,, \tag{29}$$

where $\alpha = \kappa_f/\kappa_{Na} \simeq 0.397$, $\beta = (\alpha-1)/(\alpha+2) \simeq -0.251$, and $\phi = 0.6$, the volume fraction occupied by fuel in settled paste. Above 711°K, the thermal conductivity of uranium nitride paste remains greater than the thermal conductivity of uranium metal, 35 $\mathrm{Wm^{-1}{}^{\circ}K^{-1}}$. The thermal conductivity of uranium alloy paste, 45 $\mathrm{Wm^{-1}{}^{\circ}K^{-1}}$, remains above the conductivity of metallic fuel at all temperatures. Because $\beta < 0$, as ϕ decreases, i.e., in a fluidized bed or slurry, thermal conductivity increases. Thermal conductivity of sodium vapor is significantly less, but vapor rises through liquid coolant and carries away heat by convection instead of conduction.

As remarked above, on the basis of kinetic equations, not experiments, Stein and Kasten concluded that boiling homogeneous reactors are inherently stable and can withstand enormous transients [28]. This was verified by experiments using the SUPO reactor [32] [33, pp. 133ff].

The first additional safety mechanism proposed here is the connection between the reaction and storage regions described in Section 1 and the relationship of the gas pressures above them.

When coolant boils, it creates sodium vapor. When the temperature of sodium vapor increases, its pressure increases. Both phenomena drive fuel from the reaction region into the storage region, producing negative feedback that decreases power output. Increasing reactivity increases temperature and pressure in the reaction region, and therefore reduces the amount of fuel in the reaction region. To maintain reactivity, it is necessary to increase gas pressure above the storage region, or increase power to electromagnetic pumps. Not doing so results in reducing the amount of fuel in the reaction region, which reduces power output, which reduces the temperature and pressure in the reaction region, which allows fuel to return to the reaction region. The viscosity of settled paste results in a strongly damped system without oscillations. Equilibrium is reached quickly.

There is sufficient sodium that fuel in the reaction region is always covered with sodium. Before power output becomes sufficient to boil all the sodium, vapor pressure in the reaction region is sufficient to drive all the fuel out of the reaction region and the connector, and into the storage region. Vapor would then flow through fuel to the plenum above the storage region, where it would be condensed, and its pressure reduced, by the enormous heat capacity of the sodium pool. With reaction stopped, the reaction vessel would also be cooled by the enormous heat capacity of the sodium pool, and remaining sodium vapor therein would condense. After the sodium vapor is condensed, the reaction region is empty, the level in the storage region would be the same as in the connector, and with large particles, fuel would be settled below excess sodium.

In addition to its several redundant gas pressure control valves, all of which must actively be held closed, the storage region is fitted with several redundant emergency pressure-relief valves of the rupturing diaphragm type. One accident scenario would be for a valve that controls pressure above the reaction region to be

open, all valves that control pressure above the storage region to be closed, and all of the pressure-relief valves are blocked or have failed to rupture. This would allow fuel to flow unimpeded into the reaction region, and increase the reaction rate. To counteract this, the mechanisms that actively close the pressure control valves above the storage region are thermally connected to the reaction region. One connection might be thermal switches, such as ones with bimetallic components that have different thermal expansion rates such that they open above a certain temperature. Another connection consists of several redundant small vessels of sodium contained within the reaction region, each connected via a tube to a switch that controls power to the pressure control valves. Each switch is held closed by a spring. If the temperature increases above a predetermined level, and therefore the sodium vapor pressure within any of those vessels exeeeds a predetermined value, its switch is opened. In either case, the switches are wired in series. When one switch opens, power to the valves that control storage region pressure ceases, the valves are opened, and pressure above the storage region is released. It would be necessary for all of these devices to fail in such a way that their switches remain closed, in order for all the pressure control valves to remain closed in the event of excessive temperature.

A further line of defense consists of slugs of actively-frozen paste that separate the reaction region from additional connections to an unpressurized emergency "dump" region (not shown in Figure 1), as was used in the Molten Salt Test Reactor [49]. If power to the plugs' coolers fails, or the temperature of the reaction region becomes sufficient to overcome their coolers, or the pressure exceeds their strength, the plugs melt or break and fuel flows passively into the emergency dump region. Temperature might become excessive if, for example, a leak allows sodium vapor to escape, eventually boiling away excessive coolant without increasing pressure in the reaction region.

If an emergency dump region separate from the storage region is undesirable, rather than using gas pressure to move fuel from the storage region to the reaction region, use an electromagnetic pump, power to which is enabled by the series-connected thermal switches. With constant pump power and constant pressure within the reaction region, the level of fuel would be stable. Increasing pressure within the reaction region would drive fuel back through the pump into the storage region. Separate channels that bypass the pump would connect the actively-frozen plugs to the storage region.

Releasing boron or cadmium into the reaction region in response to excessive temperature or pressure would quench the nuclear reaction, but this would require to purify all the fuel, or at least all the sodium. In APDA-146, Blessing et al [3, §IV.I.3.b] remarked that a fluid poison might be vulnerable in a reactor accident. They recommended sintered boron carbide slugs in a hydraulic cylinder, moved by sodium; such a device would not contaminate fuel with boron.

Many of the inherent safety mechanisms of EBR-II and PRISM [50, § 6], for example the Reactor Vessel Auxiliary Cooling System (RVACS), would also be used. The maximum hypothetical accident, a complete reaction and storage vessel disruption, would have the same result as in PRISM: natural dispersion into a porous easily-cooled non-critical mass at the bottom of the sodium pool. This would be an expensive mess, but not a significant safety hazard.

8 Breeding

Early analyses of homogeneous reactors fueled with aqueous solutions [19] or particles suspended in water [10], or with liquid fuel alloys [51], indicated that breeding would be more efficient with a two-region reactor than a one-region reactor. Therefore, to breed fuel using the present concept, a blanket would be used. The blanket could be composed of small particles of fertile material through which cooled sodium flows downward. Small amounts of that material could be continuously or periodically withdrawn from the bottom of the blanket using an eductor to create a slurry.

9 Alternative balance of plant

Figure 7 shows an alternative balance of plant concept.

Theoretical calculations using equations by Shair and Cristinzio [52] (Figure 8) show that a sodium-vapor

magnetohydrodynamic (MHD) generator might have very large power density at modest magnetic field strength. With an inlet temperature of 1,400°K, inlet pressure of 1.36 atm (20 psia), and Mach number 2.0, the power density can be 1 kW/cm^3 with a magnetic field of 0.125 Tesla, and 100 kW/cm^3 with a magnetic field of 0.15 Tesla. Using lithium vapor with an inlet temperature of 1,800°K, because of its smaller atomic weight and similar first gas ionization potential, the power density would be 100 kW/cm^3 with a magnetic field of 0.0715 tesla.

If the magnets in a sodium (or lithium) vapor MHD generator can operate at the temperature within the vapor chimney, it can replace the vapor chimney heat exchanger.

Sodium vapor condenses at 1,154.7°K, and lithium vapor condenses at 1,617.2°K, so a second generator would be necessary to extract energy between that temperature and the usual power plant outlet temperature. There are several possibilities for the second generator. One is a mercury vapor MHD generator. Higher magnetic field strength is required in a mercury vapor MHD generator, about 0.325 Tesla to achieve one kW/cm^3 and 0.5 Tesla to achieve 100 kW/cm^3, because of mercury's larger atomic weight and higher first gas ionization potential. U.S. patent number 3,430,081 [53] proposes that adding a small amount of barium would increase ionization, thereby increasing power density. Mercury circulation is driven by boiling. There are no pumps. A sodium-mercury heat exchanger might be necessary because sodium and mercury combine exothermically, which might be an advantage. If mercury can safely be injected directly into sodium, the vapor entering the second MHD would be mostly mercury, with a small amount of mercury remaining with liquid sodium. Both streams can subsequently be separated by distillation [54]. It is necessary to remove mercury because ^{196}Hg and ^{199}Hg have very large neutron absorption cross sections (3,078 and 2,150 barns, respectively).

For any metal vapor MHD generator, an externally supplied electric field applied before the vapor enters the MHD generator would ionize the vapor, further increasing power density, or reducing the magnetic field required.

A second concept is to inject an inert gas or a low boiling point liquid that is immiscible with sodium, does not react with sodium, and is not decomposed at the temperature of boiling sodium, into liquid sodium leaving the sodium-vapor MHD generator, producing a liquid-sodium/gas foam to use in a two-phase MHD generator. Gas would act as an accelerant. The accelerant might be mercury, but separating mercury from sodium is more difficult than separating another accelerant. An injection pump might be needed. Argonne National Laboratory investigated two-phase MHD generators [55] [56]. It might be possible to combine both concepts into a single device by injecting accelerant into the condensation region in a larger generator.

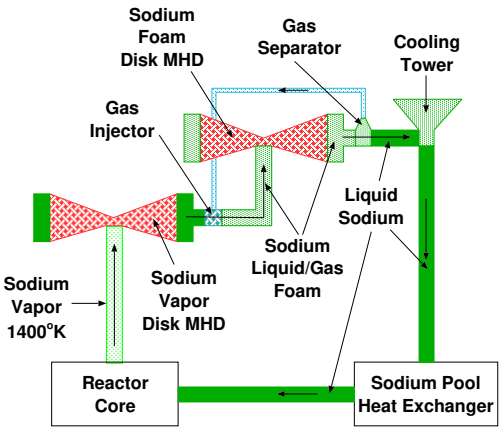

Figure 7: Balance of Plant Concept

Rather than using MHD generators, thermoelectric diodes might be used, if projected advances in efficiency occur, e.g., [57] [58].

Finally, a conventional steam system could be used. This puts water in proximity to sodium. It would require a sodium-sodium heat exchanger within the reactor to prevent radioactive sodium from entering the balance of plant, a water pump and steam generator, and a pump to supply the sodium pool heat exchanger. This is the same as in the PRISM design.

10 Alternative fuel

Reactors fueled with liquid metal alloys, primarily uranium dissolved in bismuth, with fuel circulated to an external heat exchanger, were extensively studied. Analyses by Babcock & Wilcox showed that such reactors ought to be stable against at least small oscillations at power densities up to 1,000 times greater than the nominal design level. Because the fuel was circulated to an external heat exchanger, large external fuel inventories were required. Plutonium in bismuth and plutonium in magnesium were also studied.

Pyrochemical methods to purify fuel by contact with molten NaCl-KCl-$MgCl_2$ were developed. The solubility of uranium in bismuth is very small, on the order of 0.1 wt.% at 675°K. High enrichment and a very large vessel would be required [1, Part III: Liquid-Metal Fuel Reactors]. Bismuth is corrosive to stainless steel. If the reaction were cooled by adding sodium to or flowing through the alloy, with heat removed by boiling off the sodium, this would eliminate external fuel circulation but would dilute the fuel, and perhaps make criticality impossible.

11 Conclusions

This is only a concept description, not an engineering design. There is no pretence of detailed neutronic, structural, or thermal-hydraulic analysis. The purpose of this monograph is to stimulate those analyses. There are at most two new ideas here – but the combination of ideas has not appeared. Heckman described a system using boiling sodium as a coolant in a reactor with fixed packed-bed fuel elements [20] [10, pp. 37, 46].

The inherently safe boiling-sodium reactor is compact. The concept consists of connected reaction and storage regions. It has no moving parts other than fuel and gas-pressure control valves. It has no control rods. It has no coolant circulation pumps. Operating temperature is higher, and therefore thermal efficiency is greater. Power output is controlled by the amount of fuel in the reaction region, which is controlled by the relationship of pressures above reaction and storage regions, or by an electromagnetic pump. If power to the devices that control fuel levels fails, the reaction stops because fuel flows passively from the reaction region to the storage region.

The reaction region is small. The volume of circulating primary coolant is small. Thermal inertia is small. Power output can be changed rapidly.

If electricity is produced by magnetohydrodynamic generators or thermoelectric diodes, the entire plant has essentially no moving parts.

Fuel and fertile material can be processed continuously. Very high burnup is possible. It is not necessary to shut down the reactor for refueling. The capacity factor should well exceed 95%. The "iodine pit" startup control instability is reduced or eliminated.

Auxiliary power is not needed to maintain safety during shutdown.

Details of the concept could be evaluated and refined in miniature at low cost.

References

[1] J. A. Lane, H. G. MacPherson, and F. Maslan, *Fluid Fuel Reactors: Molten Salt Reactors, Aqueous Homogeneous Reactors, Fluoride Reactors, Chloride Reactors, Liquid Metal Reactors and Why Liquid Fission*, Addison-Wesley Publishing Company, Inc., Reading, MA (1958) Library of Congress Catalog Card No. 58-12600.

[2] W. G. Blessing, J. S. Busch, J. G. Duffy, R. J. Hennig, W. H. Jens, F. W. Knight, E. C. Kovacic, D. O. Leeser, G. L. O'Neill, A. A. Shoudy, and R. G. Rateick, "Summary of the APDA Fuel Development Programs," APDA-143, Atomic Power Development Associates, 1911 First Street, Detroit, Michigan 48226 (1961).

[3] W. G. Blessing, S. D. Bowers, R. J. Hennig, P. R. Huebotter, W. H. Jens, E. C. Kovacic, F. J. Leitz, C. R. Moore, and F. P. Storrer, "Conceptual Design of a 300 MWe Paste-Fueled Fast Breeder Power Reactor," APDA-146, Atomic Power Development Associates, 1911 First Street, Detroit, Michigan 48226 (1961) https://www.osti.gov/biblio/4690257-conceptual-design-mwe-paste-fueled-fast-breeder-power-reactor.

[4] W. V. Snyder, "Finely-Divided Metal as Nuclear Power Reactor Fuel," *Nuclear Technology*, **208**, *9*, 1416 (2022) https://doi.org/10.1080/00295450.2021.2024023.

[5] E. E. Pasqualini, "Revisiting Homogeneous Suspension Reactors for Production of Radioisotopes," *14th International Meeting on Research Reactor Fuel Management*, 361–365, IAEA, European Nuclear Society, Marrakech, Morocco (2010) ISBN 978-92-95064-10-2.

[6] G. L. Hofman, L. C. Walters, and T. H. Bauer, "Metallic Fast Reactor Fuels," *Progress in Nuclear Energy*, **31**, *1/2*, 83 (1997); https://doi.org/10.1016/0149-1970(96)00005-4.

[7] T. B. Massalski, J. L. Murray, L. H. Bennett, H. Baker, and L. Kacprzak, *Binary Alloy Phase Diagrams*, American Society for Metals, Metals Park, Ohio 44073 (1986).

[8] R. S. Farr and R. D. Groot, "Close Packing Density of Polydisperse Hard Spheres," *Journal of Chemical Physics*, **131** (2009); https://doi.org/10.1063/1.3276799.

[9] E. E. Lewis, *Fundamentals of Nuclear Reactor Physics*, Academic Press (2008).

[10] C. E. Teeter, J. A. Lecky, and J. H. Martens, "Catalog of Nuclear Reactor Concepts," ANL-6892, Argonne National Laboratory, 9700 Cass Avenue, Argonne, Illinois 60440 (1964).

[11] F. Sefidvash, "Status of the Small Modular Fluidized Bed Light Water Reactor Concept," *Nuclear Engineering and Design*, **167**, 203 (1996).

[12] B. S. Triplett, E. P. Loewen, and B. J. Dooies, "PRISM: A Competitive Small Modular Sodium-cooled Reactor," *Nuclear Technology*, **178**, *5*, 186 (2012).

[13] J. K. Fink and L. Leibowitz, "Thermodynamic and Transport Properties of Sodium Liquid and Vapor," ANL-RE-95/2, Argonne National Laboratory, 9700 Cass Avenue, Argonne, Illinois 60440 (1995).

[14] F. H. Ellinger, M. N. Miner, D. R. O'Boyle, and F. W. Schonfeld, "Constitution of Plutonium Alloys," LA-3870, UC-25, TID-4500, Los Alamos Scientific Laboratory of the University of California, Los Alamos, NM (1968).

[15] U. C. Nunez, D. Prieur, R. Bohler, and D. Manara, "Melting point determination of uranium nitride and uranium plutonium nitride: A laser heating study," *Journal of Nuclear Materials*, **339**, 1 (2014).

[16] G. Junk and H. J. Svec, "The absolute abundance of nitrogen isotopes in the atmosphere and compressed gas from various sources," *Geochemica and Cosmochemica Acta*, **14**, *3*, 234 (1958); https://doi.org/10.1016/0016-7037(58)90082-6.

[17] T. Ogawa and Y. Arai, "Nitride/Pyroprocess for MA transmutation and fundamental database," Pyrochemical Separations, Avignon, France (2000).

[18] K. D. Johnson, J. Wallenius, M. Jolkkonen, and A. Claisse, "Spark plasma sintering and porosity studies of uranium nitride," *Journal of Nuclear Materials*, **473**, 13 (2016); https://doi.org/10.1016/j.jnucmat.2016.01.037.

[19] C. E. Teeter, J. A. Lecky, and J. H. Martens, "Catalog of Nuclear Reactor Concepts: Part I Homogeneous and Quasi Homogeneous Reactors: Section II Reactors Fueled with Homogeneous Aqueous Solutions and Slurries," ANL-6909, Argonne National Laboratory, 9700 Cass Avenue, Argonne, Illinois 60440 (1964).

[20] T. P. Heckman, "Fast Nuclear Reactor, Metal Vapor-He Gas Cooled," unpublished, USAEC Chicago Operations Office (1963).

[21] R. J. Rossbach and G. C. Wesling, "Two-Stage Potassium Test Turbine," NASA CR-922, General Electric (1968).

[22] E. E. Shpil'rayn, K. A. Yakimovich, E. E. Totskii, D. L. Timrov, and V. A. Fomin, *Thermophysical Properties of Alkali Metals*, Standard Press, Moscow (1970)Foreign Technology Division translator Robert A. Potts, number DTD-MT-24-120-70 https://ntrl.ntis.gov/NTRL/ document AD-721947.

[23] N. Narayana and J. Donald R. Burgess, "Melting Points and Boiling Points of Alkali Metals," NIST TN 2273, National Institute of Standards and Technology (2024); https://doi.org/10.6028/NIST.TN.2273.

[24] N. B. Vargaftik, *Tables of the Thermophysical Properties of Liquids and Gases*, Halsted Press Division of John Wiley & Sons, New York (1975) Translated by Robert C. Reid.

[25] J. L. Kloosterman, V. V. Glovko, H. van Dam, and T. H. J. J. van der Hagen, "Conceptual Design of a Fluidized Bed Nuclear Reactor," *Nuclear Science and Engineering*, **192**, *2*, 118 (2001); https://doi.org/10.13182/NSE01-A2227.

[26] W. J. Beek and K. M. K. Muttzall, *Transport Phenomena*, John Wiley & Sons, Hoboken, New Jersey (1977).

[27] G. Young, "Letter to Eugene P. Wigner," N-1668c (MUC-GY-31), Metallurgical Laboratory, University of Chicago (1945).

[28] J. M. Stein and P. R. Kasten, "Boiling Reactors: A Preliminary Investigation," ORNL-1062, OSTI 4338553, Oak Ridge National Laboratory (1951) Declassified 2 March 1957.

[29] J. H. Keenan and F. G. Keys, *Thermodynamic Properties of Steam Including Data for Liquid and Solid Phases*, John Wiley & Sons, Hoboken, New Jersey (1936).

[30] W. Wagner and A. Pruss, "International Equations for the Saturation Properties of Ordinary Water Substance, Revised According to the International Temperature Scale of 1990, Addendum to J. Phys. Chem. Ref. Data 16, 893 (1987)," *Journal of Physical and Chemical Reference*, **22**, 783 (1993); https://doi.org/10.1063/1.555926.

[31] A. C. Hindmarsh, "ODEPACK: A Systematized Collection of ODE Solvers," UCRL-88007, Lawrence Livermore National Laboratory (1982).

[32] R. N. Lyon, "Preliminary Report of the 1953 Los Alamos Boiling Reactor Experiments," CF-53-11-65, Oak Ridge National Laboratory (1953) Declassified 14 February 1957.

[33] R. E. Aven and G. T. Trammell, "Homogeneous Reactor Project Quarterly Progress Report," ORNL-1221, Oak Ridge National Laboratory (1951).

[34] M. Petrick and J. F. Marchaterre, "A Preliminary Design Study of a Boiling Slurry Reactor Experiment," ANL-6148, Argonne National Laboratory, 9700 Cass Avenue, Argonne, Illinois 60440 (1960).

[35] M. Petrick and J. F. Marchaterre, "Boiling Slurry Reactor and Method of Control," 3,088,895, U.S. Patent and Trademark Office (1963).

[36] G. A. Freund, J. D. Lokay, G. C. Milak, and J. C. MacAlpine, "Terminal Report on the Boiling Slurry Reactor Experiment (SLURREX)," ANL-6248, Argonne National Laboratory, 9700 Cass Avenue, Argonne, IL (1960).

[37] H. M. Busey, "Nuclear Reactor with a Slurry of Particles," 1,214,803, Federal Republic of Germany Patent Office (1966).

[38] T. M. Rymarz, "Studies of UO_2-NaK Slurries," ARF 3124-1, Armour Research Foundation of Illinois Institute of Technology, Chicago, IL (1960).

[39] C. S. Abrams and L. C. Witbeck, "Sodium Waste Technology: A Summary Report," ANL-86-50, Argonne National Laboratory – West, 9700 Cass Avenue, Argonne, Illinois 60440 (1987).

[40] C. E. Till and Y. I. Chang, *Plentiful Energy: The Story of the Integral Fast Reactor*, CreateSpace (2011).

[41] "RSICC Computer Code Collection – ORIGEN 2.2," ORNL/CCC-371, Oak Ridge National Laboratory (2002) https://www.wipp.energy.gov/Library/CRA/CRA-2014/References/Others/ORNL_2002_ORIGEN2_V2_2.pdf.

[42] W. V. Snyder, "Revisiting Mobile Paste Reactor Fuel," *Nuclear Technology*, **209**, *11*, 1840 (2023); https://doi.org/10.1080/00295450.2023.2205551.

[43] C. W. Forsberg, "Rethinking High-Level Waste Disposal: Separate Disposal of High-Heat Radionuclides (^{90}Sr and ^{137}Cs)," *Nuclear Technology*, **131**, *2*, 252 (2000); https://doi.org10.13182/NT00-A3115.

[44] H. H. Hausner and J. L. Zambrow, "The Powder Metallurgy of Uranium," Nuclear Engineering and Science Congress (1955) https://apps.dtic.mil/dtic/tr/fulltext/u2/a316067.pdf.

[45] T. Sofu, "A Review of Inherent Safety Characteristics of Metal Alloy Sodium-Cooled Fast Reactor Fuel Against Postulated Accidents," *Nuclear Engineering Technology*, **47**, 227 (2015).

[46] C. Hin, D. Morgan, J. Yu, and C. Papesh, "Thermal Conductivity of Metallic Uranium," NEUP 14-6767, Virginia Tech (Undated).

[47] S. B. Ross, M. S. El-Genk, and R. B. Matthews, "Thermal conductivity for uranium nitride fuel between 10 and 1923 K," *Journal of Nuclear Materials*, **151**, *3*, 318 (1988).

[48] D. J. Jeffrey, "Conduction through a random suspension of spheres," *Proceedings of the Royal Society of London Series A Mathematical and Physical Sciences*, **335**, *1602*, 355 (1973); https://doi.org/10.2307/78573.

[49] M. W. Rosenthal, P. R. Kasten, and R. B. Briggs, "Molten-salt reactors – History, status, and potential," *Nuclear technology*, **8**, *2*, 107 (1969).

[50] "Demonstration Sodium-Cooled Fast Reactor GE-PRISM," 003N4516, Rev. 2, GE/Hitachi (2016).

[51] C. E. Teeter, J. A. Lecky, and J. H. Martens, "Catalog of Nuclear Reactor Concepts: Part I Homogeneous and Quasi Homogeneous Reactors: Section IV Reactors Fueled with Liquid Metals," ANL-7138, OSTI 4539024, Argonne National Laboratory, 9700 Cass Avenue, Argonne, Illinois 60440 (1966).

[52] D. H. Shair and F. Cristinzio, "Theoretical Performance for MHD Generators Utililizing non-Equilibrium Ionization in Pure Alkali Metal Vapor Systems," R62SD94, General Electric Missile and Space Division (1963).

[53] B. Zauderer, "Mercury Vapor for Magnetohydrodynamic Generators," (1964) U. S. Patent number 3,430,081.

[54] G. Pirlot, "Method of Extracting Sodium from Amalgams," (1957) U. S. Patent number 2,798,803.

[55] M. Petrick, G. Fabris, E. S. Pierson, A. K. Fischer, C. E. Johnson, P. Gherson, P. S. Lykoudis, and R. E. Lynch, "Experimental Two-Phase Liquid-Metal Magnetohydrodynamic Generator Program," ANL-MHD-79-1, Argonne National Laboratory, 9700 Cass Avenue, Argonne, Illinois 60440 (1979) Office of Naval Research, Order No. N00014-78-F-0004, Task No. NR-099-404.

[56] M. Petrick and K.-Y. Lee, "Performance Characteristics of a Liquid Metal MHD Generator," ANL-6870, Argonne National Laboratory, 9700 Cass Avenue, Argonne, Illinois 60440 (1964).

[57] S. Kauzlarich, J.-P. Fleurial, and S. Bux, "New Materials for High Temperature Thermoelectric Power Generation," 49-2012 CFP Abstract 3714, Argonne National Laboratory, 9700 Cass Avenue, Argonne, Illinois 60440 (2012) https://neup.inl.gov/SiteAssets/2012 R_D Abstracts/49-2012_CFP_Abstract_3714.pdf.

[58] J. Gainza, S. Moltó, F. S. Sánchez, O. J. Dura, M. T. Fernández-Diaz, N. Biškup, J. L. Martinez, J. A. Alonso, and N. M. Nemes, "SnSe:K_x Intermetallic Thermoelectric Polycrystals Prepared by Arc-Melting," *Journal of Material Science*, **57**, 8489 (2022).

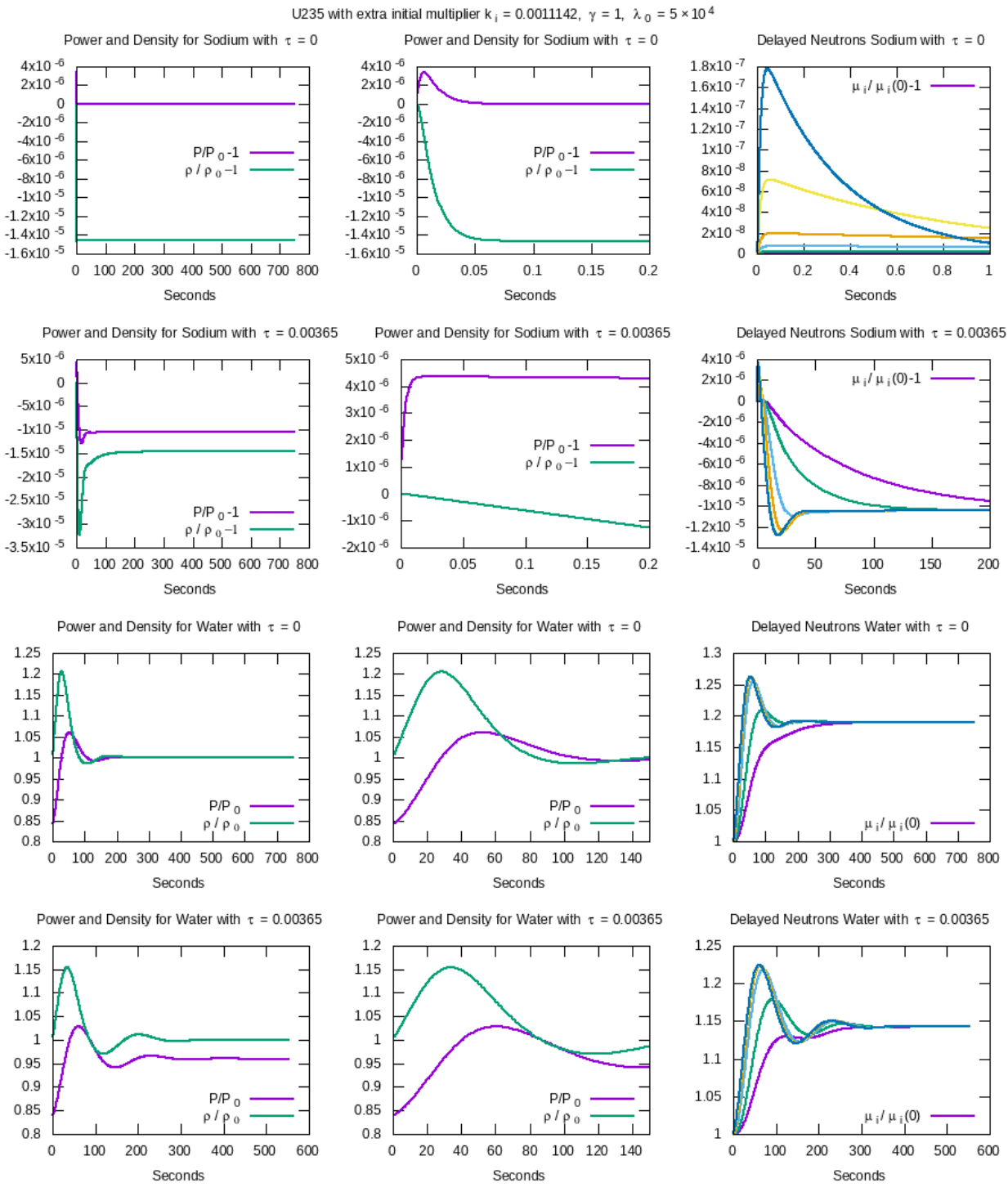

Figure 3: Solutions of the thermodynamic and kinetic equations with constant reactivity k

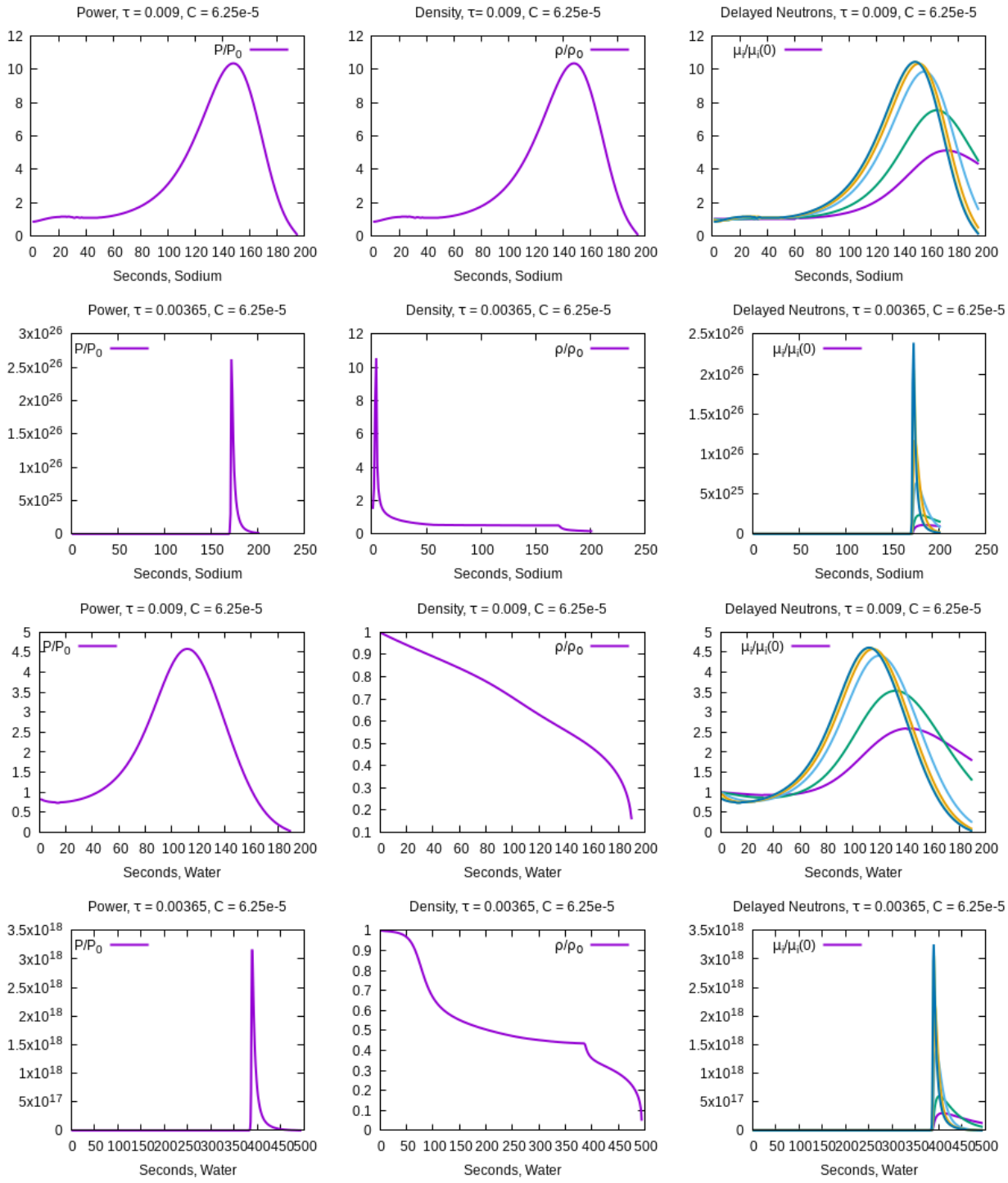

Figure 4: Solutions of the thermodynamic and kinetic equations with linearly increasing reactivity k

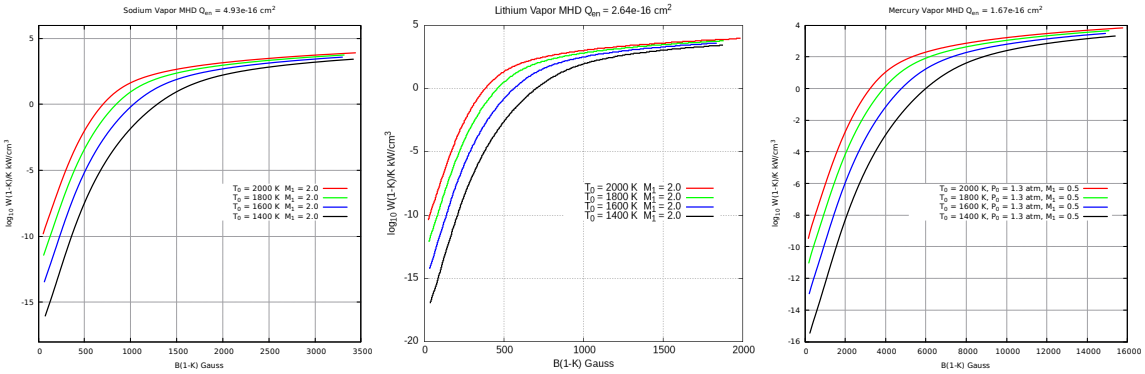

Figure 8: Magnetohydrodynamic generators' theoretical power densities ($K = E_{\text{load}}/E_{\text{open circuit}}$)